Journal of The
Electrochemical Society

Review—Graded Catalyst Layers in Hydrogen Fuel Cells - A Pathway to Application-Tailored Cells

To cite this article: Marc Ayoub *et al* 2024 *J. Electrochem. Soc.* **171** 094503

Journal of The Electrochemical Society, 2024 **171** 094503

Review—Graded Catalyst Layers in Hydrogen Fuel Cells - A Pathway to Application-Tailored Cells

Marc Ayoub,[1,2] Thomas Böhm,[1] Markus Bierling,[1,2] Simon Thiele,[1,2] and Matthew Brodt[1,*,z]

[1]*Helmholtz-Institute Erlangen-Nürnberg for Renewable Energy (IET-2), Forschungszentrum Jülich GmbH, 91058 Erlangen, Germany*
[2]*Department of Chemical and Biological Engineering, Friedrich-Alexander-Universität Erlangen-Nürnberg, Erlangen, Germany*

During steady-state operation, the proton conduction profile and the concentration profiles of the reactants and products transported through catalyst layers are non-uniform in the in-plane and through-plane directions. It is, therefore, a reasonable hypothesis that the optimal arrangement of the constituents of the catalyst layers should also be non-uniform. One way to address the non-uniformity is through graded catalyst layers. This study elucidates the state-of-the-art for graded catalyst layers, which so far were primarily investigated for proton exchange membrane fuel cells (PEMFCs). We identify the most impactful types of gradients in the PEMFC cathode and highlight studies displaying their merits in terms of better conversion efficiencies and longer lifetimes. Furthermore, two critical issues that have received little attention so far are emphasized: on the one hand, industrially relevant manufacturing techniques must be developed and implemented. On the other hand, suitable techniques are needed to identify and characterize the gradients. In this study, guidance to navigate both of these challenges is offered.
 [DOI: 10.1149/1945-7111/ad73a7]

Manuscript submitted April 11, 2024; revised manuscript received July 27, 2024. Published September 12, 2024.

Hydrogen is an essential energy carrier for the transition to renewable energy. Its production from water electrolysis and usage in fuel cells promises an environmentally-friendly energy cycle. Key technologies for the electrochemical conversion systems are proton exchange membrane water electrolyzers (PEMWEs) and fuel cells (PEMFCs). As a matter of fact, most zero-gap electrolyzers installed today are PEMWEs, and they are projected to remain so until 2030.[1,2] PEMFCs are also currently the most used type of fuel cells due to their relevance in portable, stationary, and transport applications.[3–5] Despite the projections and current applications, these systems still have research and optimization potential.[6,7] For example, it has been demonstrated for the PEMFC system that tailored catalyst layers can significantly improve the performance and durability while reducing costs.[8] One approach to tailor catalyst layers is the spatial variation of the chemical composition, which ultimately results in graded coated layers. Graded catalyst layers are the focus of this study and are investigated in the context of the PEMFC system as it is the system used for nearly all existing studies on graded catalyst layers.

The heart of a PEMFC unit is the membrane electrode assembly (MEA), as depicted in Fig. 1, which comprises the anode and cathode catalyst layers (CLs) on opposing sides of a proton exchange membrane (PEM). The MEA is sandwiched between the gas diffusion layers (GDLs). The hydrogen oxidation reaction (HOR) occurs at the anode, splitting hydrogen into protons and electrons. Electrons travel from the anode to the cathode through an external electrical circuit, while the protons pass through the membrane to the cathode. The oxygen reduction reaction (ORR) occurs at the cathode, forming water. The ORR is typically 6 orders of magnitudes slower than the HOR.[9–11] As a result, the cathode requires higher catalyst loadings, often based on platinum group metals (PGMs). Thus, catalyst activity and utilization are important economic factors.

During fuel cell operation, inhomogeneous profiles form for the oxygen concentration, ionic potential, catalytic activity, and temperature. For example, the oxygen concentration decreases in the cathode towards the membrane and gas outlet, as it is being consumed. Due to the lower O_2 concentration, the turnover frequency of the catalyst towards the membrane and gas outlet also decreases. An uneven catalytic activity would also mean an uneven temperature generation. Contrary to the O_2 concentration profile, the proton conduction profile decreases from the membrane interface towards the cathode electrode. This profile is also dependent on the proton conductive ionomer used and the relative humidity (RH) during operation. Due to these inherent profiles and anisotropies that form within electrodes during fuel cell operation, a preferential distribution of the chemical constituents becomes worthy of consideration. An adapted electrode design with gradients that compensate for reactant concentrations could result in lower costs by reducing the platinum group metals (PGM) catalyst loading while maintaining the performance in the high current density regime or improving the performance at equal PGM loading.[12,13] Furthermore, homogenizing the reaction rates and current distribution along the MEA via graded CLs can reduce degradation hotspots and improve the durability of a PEMFC.[14–17] In some scenarios, graded catalyst layers can also enhance the performance at different operating RHs.[18]

Xing et al. laid out a groundwork review on gradients in PEMFCs that gave an essential overview of graded GDLs, MPLs, and CLs.[19] In this work, we focus exclusively on graded cathode CLs for PEMFCs, and cover many previously unexplored areas: (i) Insights on naturally occurring gradients are provided, (ii) Suitable analysis strategies to detect the gradients are recommended, (iii) Up-to-date experimental and modeling results are discussed clarifying discrepancies encountered in the studies, (iv) Uninvestigated gradient types, which can also reduce catalyst dissolution problems, are also touched on, (v) An assessment of suitable manufacturing techniques for creating gradients is presented. Particularly the latter is significant as the more complex manufacturing process is one main obstacle inhibiting the introduction of graded structures in high-throughput manufacturing.

Review on Graded Catalyst Layers

Introduction of a precise notation.—The interactions among chemical constituents in graded catalyst layers can be complex; often the grading of one chemical constituent results in the grading of the remaining chemical constituents. For example, a through-plane ionomer solid loading content gradient increasing towards the membrane typically results in a through-plane catalyst solid content

*Electrochemical Society Member.
[z]E-mail: ma.brodt@fz-juelich.de

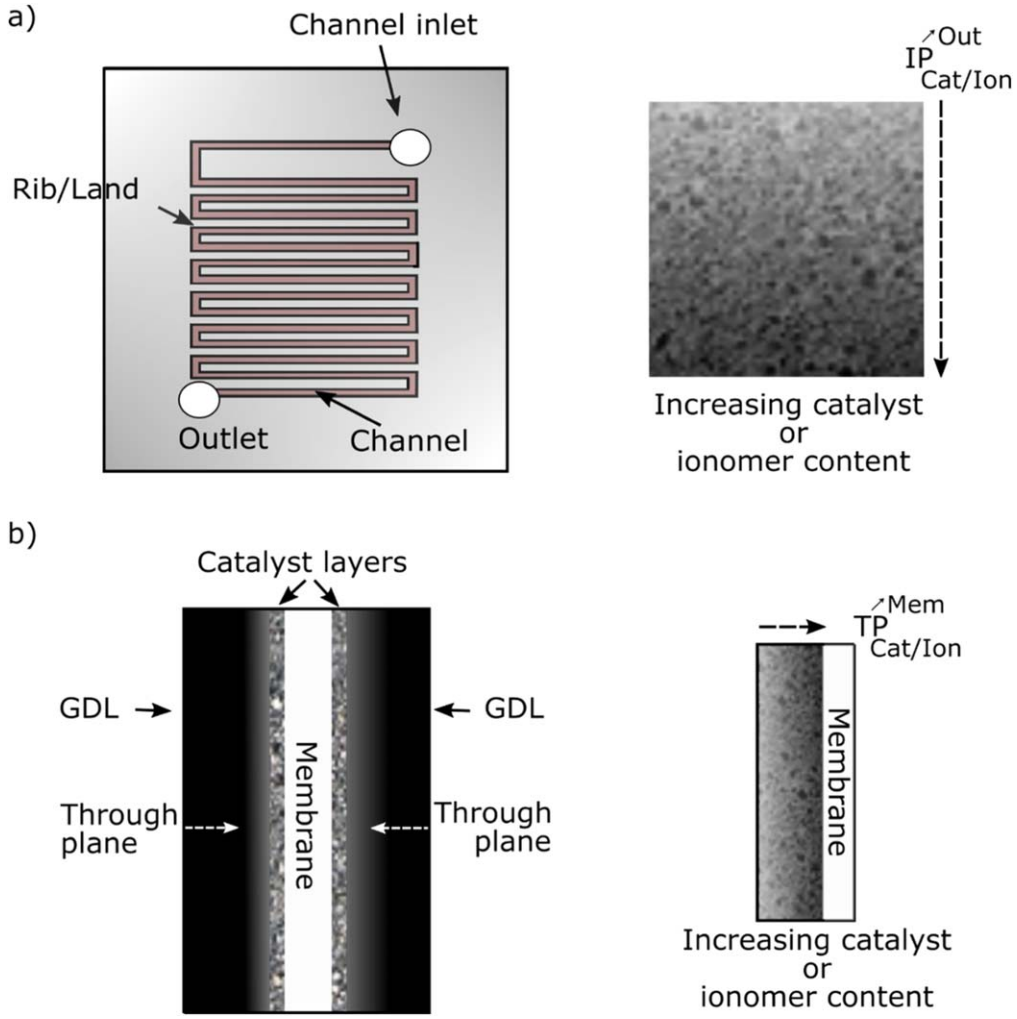

Figure 1. (a) An illustration of flow-fields showing the inlet and the outlet for the reactants and products, with an example of an in-plane gradient. (b) Through-plane illustration of an MEA showing the GDL, catalyst layers, and membrane with an example of a through-plane gradient for the catalyst layer.

gradient increasing towards the GDL. Additionally, different layers can have different thicknesses depending on the catalyst gravimetric loadings of the coated layers, due to the packing density of the carbon support, which is primarily responsible for the dry film thickness.[20,21] This also means that an ionomer loading/solid content gradient results in interparticular pore size gradients. To address this interplay and prevent confusion, a notation to describe gradients precisely is provided below.

We introduce a clear notation to address this complexity, which we will use throughout the text. Gradients in catalyst layers can be oriented in the through-plane (TP) and also in-plane (IP) directions (Fig. 1). For the TP direction, the catalyst loading or ionomer solid content can increase either towards the membrane or towards the GDL. In the IP direction, the solid contents can increase or decrease towards the inlet or outlet, towards the channel or the land. Hence, to address the gradients we introduce the following notation, $X_Y^{\nearrow Z}$ to precisely describe them:

$$X_Y^{\nearrow Z}: \begin{cases} X, & \text{either the IP or TP direction} \\ Y, & \text{the graded element(e.g., ionomer or catalyst solid contents(ion/cat))} \\ Z, & \text{the increasing grading direction(e.g., higher to membrane or outlet(mem/out)} \end{cases}$$

For example, $TP_{Ion}^{\nearrow Mem}$ would denote a gradient in the through-plane direction with an increasing ionomer content towards the membrane.

There can also be combinations of both grading directions: for example, an MEA with two coated layers can have a through-plane gradient, e.g. $TP_{Ion}^{\nearrow Mem}$ and within each layer, there can be in-plane gradients (e.g. $IP_{Cat}^{\nearrow Out}$). Such a concatenation of gradients would be described as: $TP_{Ion}^{\nearrow Mem} \cdot IP_{Cat}^{\nearrow Out}$. Finally, we would like to highlight that most available studies use two coated layers, and only a few studies use three-coated layers. Thus, annotations for two- and three-coated layers are also presented for this study, DCLs for double-coated layers, and TCLs for triple-coated layers.

Literature survey on graded catalyst layers.—In the following, we provide a systematic overview of literature works on graded layers for the cathode of hydrogen fuel cells. First, TP gradients are examined followed by IP gradients. Each subsection starts with available

modeling results followed by the experimental ones. The gradients used for these sections are $TP/IP_{Ion}^{\nearrow Mem/GDL}$, $TP/IP_{Cat}^{\nearrow Mem/GDL}$, $TP/IP_{Binder}^{\nearrow Mem/GDL}$, $TP/IP_{Pore\ Size}^{\nearrow Mem/GDL}$, and $TP/IP_{Particle\ Size}^{\nearrow Mem/GDL}$ gradients. Pore-size gradients typically form with other gradients, such as $TP_{Ion}^{\nearrow Mem/GDL}$. Therefore, $TP_{Pore\ Size}^{\nearrow Mem/GDL}$ gradients are not mentioned in a separate section, especially as these were not explicitly tailored for CLs yet.

Naturally occurring ionomer gradients.—An often overlooked and less investigated topic is naturally occurring gradients, i.e., gradients that are not added voluntarily but form naturally from coating and drying procedures within single layers. We slightly touch on this topic, before further studying intentionally graded electrodes. Cleve et al.[22] showed that variations in electrode inks' water-to-alcohol ratio lead to different ionomer distributions in spray coated catalyst layers.[22] A water-rich ink led to higher ionomer concentrations on the surface. Other influencing factors for the self-organization processes of the materials during film formation include the agglomeration tendency of particles, the drying rate, and the particle size distribution.[23–25] Mauger et al. systematically investigated the influence of ink formulation and drying conditions on ionomer distribution in roll-to-roll-coated gas-diffusion electrodes for PEMFCs.[23] The authors observed that a water-rich catalyst ink and a higher drying temperature promoted homogeneous ionomer-rich surfaces. On the contrary, a 1-propanol-rich ink led to lower concentrations of the ionomer on the surface and displayed more irregularities.

Intentional ionomer TP gradients.—Typically, the proton transport rate in the cathode is highest close to the membrane interface and decreases to the GDL as protons are consumed (Fig. 2).[26,27] Therefore, it is intuitive to consider electrode designs with a high ionomer content close to the membrane. However, an excessive ionomer content in any part of the electrode can limit oxygen transport, favor cathode flooding, and electrically insulate some catalytic sites. Also, the conductivity of an ionomer is dependent on relative humidity in the cell.[28] Thus, the optimum ionomer gradient becomes application-dependent as different applications often have diverse operating conditions.

Xing et al. presented a numerical study illustrating the importance of the operating conditions and overall loadings on the gradient distribution.[30] The authors found that the optimum slope (gradient steepness) depends on the current density. Operations at low current densities (above 0.60 V) achieve a maximum performance when the catalyst and ionomer are uniformly distributed (i.e., without a gradient). Operations at medium and high current densities (0.60 V and below) achieve a maximized performance when graded CLs are used.[30] A $TP_{Ion}^{\nearrow Mem}$ gradient with a high steepness can result in enhanced proton conductivity and mass transport properties as long as the agglomerates remain interlinked and form an electrically conductive structure and interparticular pore volumes for the transport of oxygen aren't critically reduced.[30] Wang et al.'s model also predicted that introduction of a $TP_{Ion}^{\nearrow Mem}$ gradient (TCL) slightly improves fuel cell performance compared to non-graded samples due to enhanced mass transport properties and proton conduction.[31] Contrarily, a $TP_{Ion}^{\nearrow GDL}$ TCL can lower the performance due to poorer mass transport and proton conduction properties.[31] Wang et al. verified their model experimentally. Their results are displayed in Fig. 3.[32] The improved performance (550 mW cm^{-2} vs 460 mW cm^{-2}) for the $TP_{Ion}^{\nearrow Mem}$ gradient was attributed to enhanced proton conduction at the membrane interface and enhanced mass transport properties near the GDL.[32] Equal layer thicknesses were observed with high-resolution TEM imaging, which confirm the presence of an interparticular $TP_{Pore\ size}^{\nearrow GDL}$ gradient for the TCLs. In another experimental study, Kim et al., reported DCLs with $TP_{Ion}^{\nearrow Mem}$ with improved performance due to enhanced mass transport properties.[13] These DCLs also had layers with similar thicknesses,

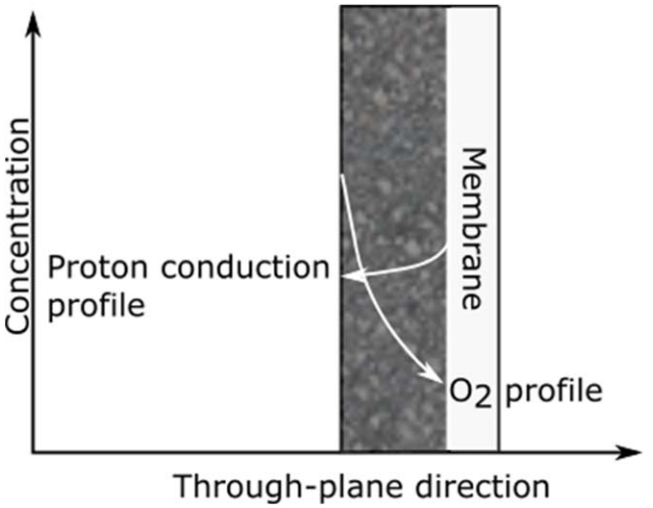

Figure 2. Possible proton and oxygen transfer profiles in the TP direction for non-graded catalyst layers.[26,29]

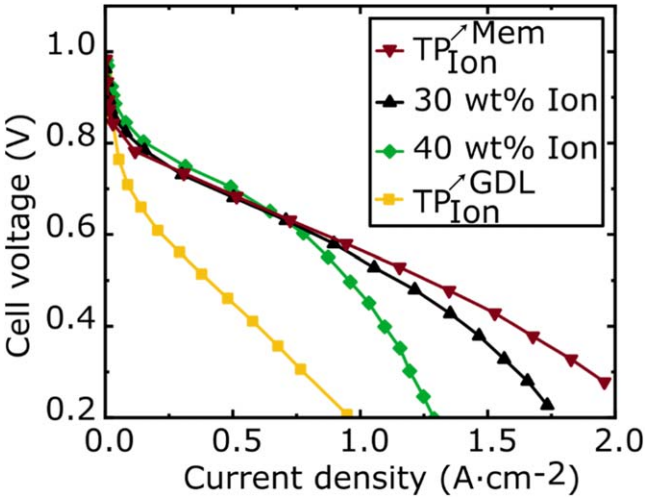

Figure 3. Experimental comparison of GDEs with and without gradient at 75 °C, 101.325 kPa, and over-humidified conditions.[32] Figure republished from Journal of the electrochemical society (JES).

confirming again the presence of interparticular $TP_{Pore\ size}^{\nearrow GDL}$ gradients. When a too-low ionomer content close to the GDL (10 wt%, I/C: 0.28) for the $TP_{Ion}^{\nearrow Mem}$ DCL was used, the performance became worse due to impaired proton conduction and reduced electrochemical surface area (ECSA). This experimental finding confirms the requirement presented by Xing et al. of an ionomer interlinked agglomerate network for enhanced performances.[30] Chen et al. showed that a $TP_{Ion}^{\nearrow Mem}$ DCL can improve the peak power density by 25.4% at 80% RH compared to a non-graded cell.[18] At a low RH of 20%, the improvement in peak power density became 104.2%. This significant increase in peak power density at lower RH suggests that $TP_{Ion}^{\nearrow Mem}$ gradients are particularly beneficial at low RHs. However, it is not clear if the reference non-graded electrode had the optimum I/C ratio at the tested low relative humidity. Nevertheless, the improvements were attributed to enhanced mass transport properties and better proton conductivity due to an increased water content at the electrode-membrane interface. $TP_{Ion}^{\nearrow Mem}$ gradients are also in discussion for flourine-free systems, however, no clear trends could be derived yet, and further research is required.[33]

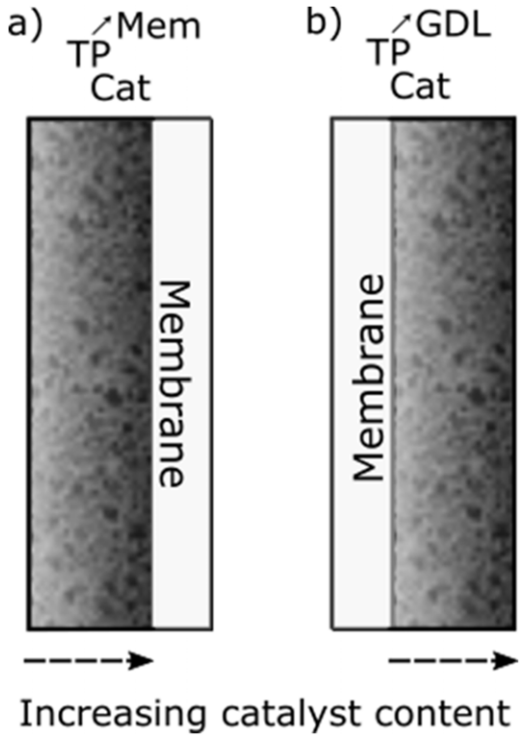

Figure 4. Preferable catalyst distribution in the TP direction: (a) Increasing towards the membrane, or (b) increasing towards the GDL.

The present studies indicate that a $TP_{Ion}^{\nearrow Mem}$ gradient in the cathode, which also results in interparticular $TP_{Pore\ size}^{\nearrow GDL}$ gradients, can have an advantageous impact on the cell performance. The I/C ratios used for the gradients shouldn't be far from the optimal I/C ratio for the non-graded cathodes. Even with the correct gradient direction, performance may be worse if the steps/slopes are too large. For example, Yoon et al. found that a CL with 35 wt% (I/C: 0.9) Nafion™ uniformly distributed outperformed DCLs with 10 wt % (I/C: 0.37) and 60 wt% (I/C: 2.5) of Nafion™ in both directions.[34] The expected operating conditions must be taken into account when considering the choice of gradient and the overall electrode design. For example, Shahgaldi et al. achieved a similar performance with lower total ionomer loadings with $TP_{Ion}^{\nearrow Mem}$ gradients under fully humidified conditions compared to MEAs with CLs without gradients.[35] Chen et al. noticed that the improvements of $TP_{Ion}^{\nearrow Mem}$ gradients become more expressed at lower RH. Thereby, a $TP_{Ion}^{\nearrow Mem}$ can enhance the proton conduction and the reactant transfer processes. Also, the kinetic region shows differences in the polarization curve, especially at low relative humidities.[18] Under high relative humidities, no apparent differences are visible between MEAs with homogenous CLs and $TP_{Ion}^{\nearrow Mem}$ gradients in the activation regions.[18,32,33] However, $TP_{Ion}^{\nearrow GDL}$ gradients resulted in more significant losses in the activation region.[32] At low RH, the kinetic features became more distinguishable, favoring $TP_{Ion}^{\nearrow Mem}$ gradients. One explanation could be that the $TP_{Ion}^{\nearrow Mem}$ gradient increases the local water content in the MEAs, which also aids the catalytic activity.[36–38] However, to confirm if the impact directly affects the kinetic activity, one needs to analyze internal resistance (IR)-corrected polarization curves and further analyze the results. This can be challenging since the protonic resistance of the catalyst layer is required for an IR correction, which is usually extracted from impedance models. Because standard transmission line impedance models assume homogenous conditions throughout the catalyst layer are non-suitable for graded catalyst layers, more advanced models must be used.[27]

Catalyst loading TP gradients.—Inferring a clear trend on the preferential distribution of the catalyst is a non-straightforward task. Some studies claim a $TP_{Cat}^{\nearrow Mem}$ gradient is advantageous, whereas others claim a $TP_{Cat}^{\nearrow GDL}$ is favorable. With the help of the RH, water management, and reactant transport mechanisms, a reasonable explanation to the contradictory results encountered in the literature is presented.

We start by discussing the studies favoring $TP_{Cat}^{\nearrow Mem}$ gradients (Fig. 4a). A numerical study by Song et al. found that a $TP_{Cat}^{\nearrow Mem}$ gradient enhances mass transport properties and results in increased catalyst utilization.[39] Similarly, Jain et al. and Cetinbas et al. numerically found a $TP_{Cat}^{\nearrow Mem}$ to be beneficial with regards to maximized performance.[40,41] In an agglomerate model, Roshandel et al. found that a $TP_{Cat}^{\nearrow Mem}$ gradient also improved the performance due to higher local reaction rates.[42] Kim et al. confirmed this trend is an experimental study where $TP_{Cat}^{\nearrow Mem}$ gradients in conjunction with fixed $TP_{Ion}^{\nearrow Mem}$ gradients were found to enhance the performance (by $\sim 25-30\%$) due to better mass transport and water management properties.[13] A $TP_{Cat}^{\nearrow GDL}$ gradient was not investigated. Another experimental study favoring $TP_{Cat}^{\nearrow Mem}$ gradients was reported by Chen et al. where gradients were made by varying the Pt/C ratios of the coated layers.[18] A higher Pt/C ratio at the membrane interface resulted in a 32.1 % improved peak power density at 80 % RH while an opposite gradient resulted in worse performances compared to a non-graded sample. At 20 % RH, the same $TP_{Cat}^{\nearrow Mem}$ gradient resulted in 82.7 % improved power density. The authors attributed these improvements to higher Pt utilization and reduced mass transfer losses.[18] Similarly, Su et al. also studied $TP_{Cat}^{\nearrow Mem}$ gradients by varrying the Pt/C ratios in the coated layers.[43] They found improved performances (from 580 mW cm^{-2} to 660 mW cm^{-2}) for the gradients compared to a non-graded sample due to better mass transport properties and higher platinum utilization efficiency.[43]

Next, we investigate the studies favoring $TP_{Cat}^{\nearrow GDL}$ gradients (Fig. 4b). Then we offer a possible explanation for the discrepancies encountered. Most aforementioned numerical models are based on continuum mechanics, where all the catalyst particles form triple phase boundaries.[19] Higher platinum loadings near the GDL improved the performance when two-phase flows (liquid and gaseous) were considered. Srinivasarao et al. used a spherical two-dimensional agglomerate model that considered two-phase flows and found that the optimum Pt distribution takes the form of a $TP_{Cat}^{\nearrow GDL}$ gradient at high current densities and medium voltages (around 0.5 V). The improvements were attributed to improved mass transport properties.[44] Similarly, Xing et al. accounted in their model two-phase flow mechanisms and found a $TP_{Cat}^{\nearrow GDL}$ gradient to be beneficial for the performance.[19,30] Xing et al. also observed that the optimal gradient shape is strongly influenced by the overall loading and the operating conditions.[44,45] This outcome is consistent with the findings of Secanell et al., who concluded that different operating conditions have different preferential catalyst layer compositions.[46,47] Interestingly, only one experimental study so far confirms this trend.[33] Nguyen et al. found that a $TP_{Cat}^{\nearrow GDL}$ gradient in a DCL with 25% of the total cathode catalyst in the layer close to the membrane with an I/C ratio of 0.2 (10 wt% flourine-free ionomer) and 75% close to the GDL with an I/C ratio of 0.4 (18 wt% flourine-free ionomer) resulted in an improved performance compared to a non-graded one at 50 % and 80 % RH.[33] The graded sample showed a better balance in the ECSA, mass activity, activation losses, proton conduction, and mass transport properties than other gradients and non-graded samples.

To understand the discrepancies in the literature regarding the optimal grading direction, it is helpful to anticipate the water profiles at different current densities. It is well known that at high current densities, produced water can hinder oxygen diffusion into the

catalyst layer. As a result, the reaction zone shifts away from the membrane interface due to mass transport limitations. In that case, the $TP_{Cat}^{\nearrow GDL}$ gradient could be beneficial. However, the proton conduction is a limiting factor in that case because the protonic conduction is highest close to the membrane interface. Therefore, a performance improvement at high current densities due to a $TP_{Cat}^{\nearrow GDL}$ gradient becomes an interplay between better mass transport properties and higher protonic resistances. These opposing factors explain the discrepancy in the literature regarding $TP_{Cat}^{\nearrow GDL}$ gradients. In the study by Chen et al. where current densities greater than $2 A cm^{-2}$ were achieved, different Pt/C ratios were used to make the gradients.[18] This should theoretically have resulted in thinner catalyst layers for the same Pt loading, which drastically affect the diffusion rate. In the study by Nguyen et al., a sulfonated phenylated polyphenylene (PPP) ionomer was used, a non-conventional ionomer type compared to the common PFSA ionomer, $IEC = 3\ m_{eq}\ g^{-1}$; $EW \approx 333$. This low EW ionomer likely retains reasonably low proton resistance at (close to) cathode flooding conditions, which resulted in an overall increase in fuel cell performance. In summary, different operation conditions result in different optimum gradient structures for the catalyst distribution. At lower current densities with no cathode flooding, $TP_{Cat}^{\nearrow Mem}$ gradients are likely favored to compensate for the lower oxygen concentration at the membrane interface. At high current densities, the optimum grading direction varies and becomes application and material dependent.

TP gradients as a means for degradation mitigation.—The influence of gradients on MEA degradation has been scarcely addressed in the literature. For example, only a few research groups studied catalyst dissolution in an MEA with a TP gradient. However, dissolution mitigation through graded layers might be worth further investigation based on their potential benefits.

A mathematical model by Zheng et al. displays such potential benefits where the catalyst durability was enhanced with the incorporation of $TP_{Particle\ size}^{\nearrow Mem}$ gradients. Modeling results for a DCL suggest that $TP_{Particle\ size}^{\nearrow Mem}$ gradients with larger Pt particle sizes, about 4–5 nm near the membrane, could mitigate ECSA losses by 33 to 55 % compared to particle sizes of 3 nm. This could, however, accelerate the Pt dissolution at the GDL interface, despite reducing the Pt dissolution at the membrane interface. To counterbalance this effect, a TCL with a smoother $TP_{Particle\ size}^{\nearrow Mem}$ gradient transition (5-4-3 nm) was recommended, along with a $TP_{Cat}^{\nearrow GDL}$ gradient.[14] Yu et al. experimentally verified the improvements of a $TP_{Particle\ size}^{\nearrow Mem}$ gradient by catalyst dissolution accelerated stress tests (AST) defined by the U.S Department of Energy (DOE). Standard electrodes with Pt particle sizes of 5nm and 2nm were compared to the gradient consisting of 5nm close to the membrane and 2nm close to the GDL.[15] The performance of the MEA with the $TP_{Particle\ size}^{\nearrow Mem}$ gradient was similar to the control cells at the beginning of testing (BOT) but better by 50–100 mV at the end of testing (EOT) for the same current density. Also, the ECSA retention and the Pt loss were improved due to slower Ostwald ripening.[15,48,49] Similar results were also found in another study by the same working group.[17] Yu et al. also sprayed $TP_{Cat}^{\nearrow Mem}$ gradients based on a 2 nm Pt catalyst with Pt/C ratios of 60 wt% near the membrane and 40 wt% near the GDL.[16] The $TP_{Cat}^{\nearrow Mem}$ gradient showed higher voltages at BOT and EOT (50–100 mV) at equal current density compared to a uniform GDE with 40 wt% of Pt/C catalyst. The improvement was attributed to roughly 80–60 % less Pt dissolution in the depletion zone, 2 μm from the CL/membrane interface.[16] Compared with the $TP_{Particle\ size}^{\nearrow Mem}$ gradient, the $TP_{Cat}^{\nearrow Mem}$ gradient showed more effective degradation mitigation since a higher percentage of smaller particles (<5 nm) was retained, despite having a slightly higher Pt loss into the membrane.[16]

To the best of our knowledge, the influence of electrode gradients on other degradation mechanisms, such as carbon corrosion, has not been studied yet. Furthermore, additional studies on the degradation of a given gradient under relevant operating conditions are required.

Binder loading TP gradients.—PFSA-based ionomers are typically employed as proton-conductive binder materials. However, non-conductive binder materials can also be employed. A total replacement of the PFSA binder by a non-conductive binder will likely result in reduced performances due to a lack of proton conductivity in the electrode, but combining the two binders can potentially improve product removal at the cathode in some scenarios and enhance the mechanical strength of the MEA. The literature provides studies on PTFE as a highly hydrophobic and non-conductive binder.[50–53]

Zhao et al. were among the few authors who experimentally investigated DCLs containing PTFE for PEMFCs.[50] The DCLs were bound with PFSA close to the membrane interface and with PTFE close to the GDL interface.[50] The inner layer thickness with PFSA and the outer layer thickness with PTFE were varied, and the overall platinum loading was constant at $0.40 mg\ cm^{-2}$. The electrodes were tested under fully humidified conditions at 50 °C. Compared to a conventional electrode with a PFSA binder, a DCL with one-third of the total electrode's thickness containing PTFE as a binder close to the GDL had an increased power density by around 20%. The performance boost was attributed to enhanced hydrophobic-hydrophilic balances, improving mass transport mechanisms. A lower HFR was also obtained from electrochemical impedance measurements.[50] Lin et al. presented a further in-depth study on the influence of PTFE cathode gradients while fixing the Pt loading at $0.2 mg\ cm^{-2}$ for the cathode.[12] The authors found that applying a gradient with 10 wt% of PTFE close to the GDL ($TP_{PTFE}^{\nearrow GDL}$) resulted in improved durability by voltage cycling and performance in the high current density regime. Furthermore, a graded TCL was compared with a graded DCL. It was found not to result in significant improvements, suggesting that manufacturing a DCL is sufficient for significant improvements of roughly 30% of the maximum power density. The most significant improvements were visible at fully humidified conditions in the mass transport regime. The ohmic resistance from electrochemical impedance measurements also improved compared to uniform samples and $TP_{PTFE}^{\nearrow Mem}$ gradients.

For PTFE, most studies deal with graded GDLs, rather than graded catalyst layers. Only a handful of studies apply PTFE in the catalyst layer in such a way that it results in well-defined gradients, and no numerical studies deal with this. Considering the potential benefits, this could be an interesting avenue for further research. Besides PTFE, applying gradients with other binding polymers such as PEEK and PVC, could also be candidates for future studies.[12,54,55]

IP graded catalyst layers.—IP graded catalyst layers are meant to mitigate problems occurring along the gas channels of fuel cells (Fig. 1a). The oxygen concentration decreases towards the outlet while the water content increases. Further, there are IP concentration differences between channel and land areas within the flow field, as the gas streams only provide convective flow above the channel area. Thus, a lower ionomer and catalyst loading under the land area seems reasonable to reduce the catalyst loading without sacrificing performance. However, few experimental studies deal with such oscillatory IP gradients, presumably due to challenging manufacturing procedures. As a result, most experimental studies have focused on gradients between the inlet and outlet (Fig. 5) and disregarded the flow fields.

Roshandel et al. developed an agglomerate model that was verified with experimental data and studied the oxygen concentration and the effect of the catalyst distribution on cell performance.[42] They achieved performance improvements with $TP_{Cat}^{\nearrow Mem}$ • $IP_{Cat}^{\nearrow Air\ Channels}$

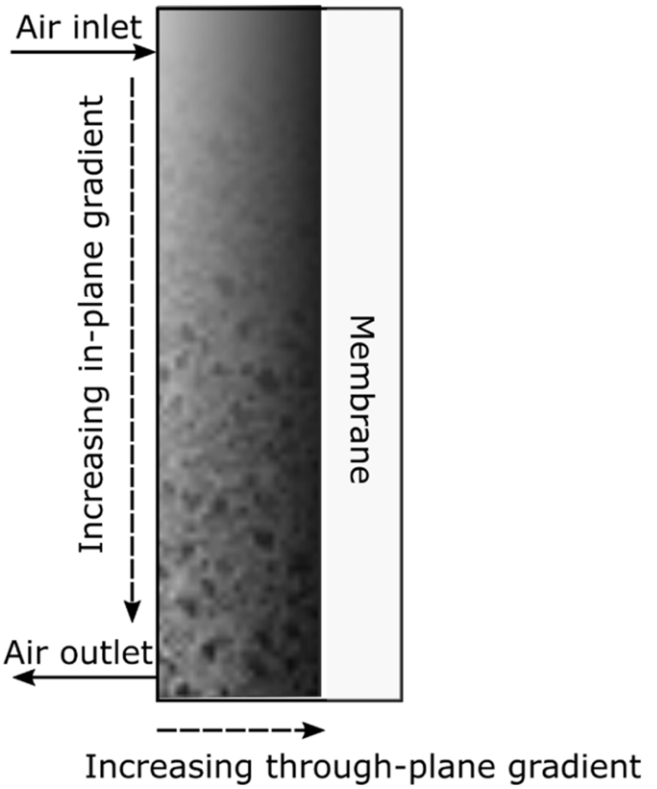

Figure 5. Combined IP and TP gradients for the cathode electrode increasing towards the membrane and outlet (e.g., catalyst loading). Air enters at the inlet and leaves with the lowest concentration in the outlet.

gradients due to higher local reaction rates.[42] A numerical study by Ebrahimi et al. found that a homogenous current density distribution does not necessarily improve the system's performance. An IP gradient in catalyst loading with a minimum necessary loading under the land area and increased loading below the channel area was recommended for enhanced performance.

Santis et al. investigated $IP^{\nearrow Out}_{Cat}$ gradients for PEMFCs with the help of a segmented cell and current density distribution measurements.[56] They found that the current density can be homogenized by increasing the catalyst loadings towards the outlet and channels.[56] A steep gradient profile was found to homogenize the current density better at an air stoichiometry of 2.0 than at higher stoichiometries. A smoother profile, in contrast, was better suited for higher air stoichiometries. However, no increase in cell performance was achieved by homogenizing the current density. Nevertheless, the lifetime could be positively influenced by avoiding significant different currents at different locations.[56] Considering the relatively high platinum loadings utilized, it is reasonable to repeat the measurements with lower state of art loadings. Prasanna et al. prepared cathodic $IP^{\nearrow Out}_{Cat}$ gradients and saw improved performances for $IP^{\nearrow Out}_{Cat}$ configurations because of increased local reaction rates towards the outlet where the oxygen concentration is lowest.[57] Compared with a uniform electrode with a platinum loading of 0.3 mg cm^{-2}, an $IP^{\nearrow Out}_{Cat}$ gradient with the same overall loading but with a distribution from 0.2 to 0.35 mg cm^{-2} resulted in about a 17% increase in the maximum power density. Zhang et al. analyzed the current density distribution in cells with $IP^{\nearrow Out}_{Cat}$ gradients using MEAs with three segments of different catalyst loadings.[58] Using a segmented current collector, they found higher performance with the IP gradient accompanied by a more homogeneous current distribution than uniform catalyst layers. The authors concluded that IP gradients can mitigate aging by preventing hot spots because of a homogeneous current distribution.[58]

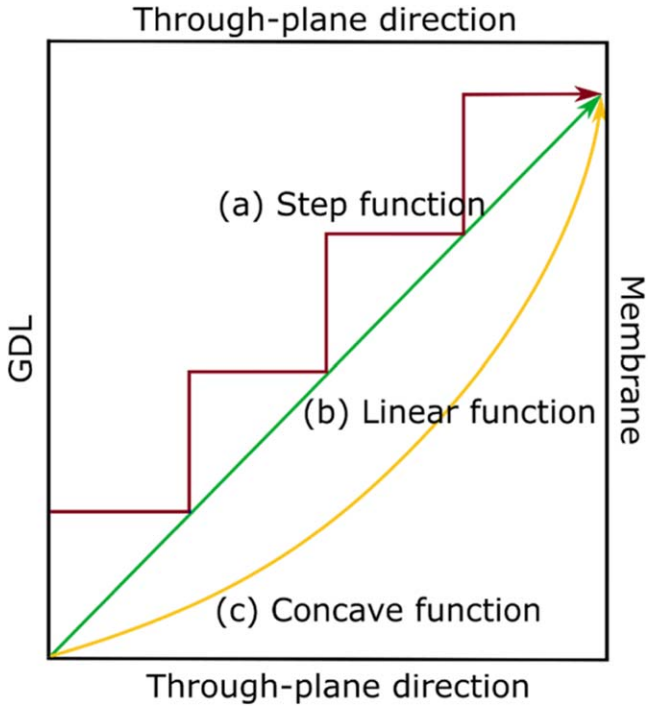

Figure 6. Examples of possible gradient functions: (a) increasing step function, (b) increasing linear function, (c) increasing concave function.

Herden et al.[59] tested $IP^{\nearrow Out}_{Ion\ EW}$ graded cathodes for PEMFCs using equivalent weights (EWs) of 772 and 825 $g_{polymer}\ \ mol^{-1}_{SO_3^{-1}}$ under varrying RHs of 33% to 100%. The I/C ratio was fixed at 0.8 and the cathode loading was maintained at 0.3 mg cm^{-2}. A uniform cathode utilizing the high EW ionomer resulted in better performance at high RHs whereas the lower EW sample resulted in better performance at low RHs. The low EW sample has a higher degree of swelling and water uptake capability than the higher EW ionomer, which explains its better performance at low RH and worse performance at high RH.[59,60] Compared to the uniform samples, an equal sized $IP^{\nearrow Out}_{Ion\ EW}$ graded cathode resulted in similar optimum performances at both low (33%) and high RHs (100%) due to an improved balance between ohmic losses and mass transport resistances.

Summary.—

- $TP^{\nearrow Mem}_{Ion}$ gradients can enhance performance due to improved proton conduction. Typically, this gradient type also results in a $TP^{\nearrow GDL}_{Pore\ size}$ gradient, which reduces mass transfer losses.
- $TP^{\nearrow Mem}_{Cat}$ gradients have been shown to improve cell performance by increasing the number of reaction sites with lower protonic resistance closer to the membrane interface. However, the oxygen concentration decreases towards the membrane, mainly when cathode flooding occurs, which would favor $TP^{\nearrow GDL}_{Cat}$ gradients. Thus, the ideal gradient depends on the operating conditions.
- $TP^{\nearrow Mem}_{Particle\ Size}$ gradients are likely to enhance the durability by improved ECSA retention and less Pt dissolution into the membrane. Smooth particle size gradients were recommended.
- A combination of $TP^{\nearrow GDL}_{PTFE}$ and $TP^{\nearrow Mem}_{Ion}$ gradients can improve mass transport properties without limiting proton conduction.
- An $IP^{\nearrow Out}_{Cat}$ gradient can improve the performance by a more effective oxygen consumption along the flow field and can also homogenize the current density distribution.

Graded catalyst layers are still a scarcely investigated topic. For example, employing binders consisting of different ionomers or EW is worth consideration, both in the IP and TP direction. Also

employing different I/C ratios for the IP direction could be worth consideration. Herden et al. found that an MEA with an $IP^{\nearrow Out}_{Ion\ EW}$ gradient resulted in a wider RH operation range.[59] A similar approach may be beneficial with increasing I/C ratios as well. Also, investigations on alternating gradients could be interesting from an experimental perspective. However, realizing such experiments in labs with small cells can be challenging.

Tailored pore size and particle size gradients are particularly interesting yet relatively unexplored topics. So far, the formed pore size gradients are governed by the binder type and content. However, catalyst inks can also contain pore-forming additives to tailor pore sizes, which could enable $TP^{\nearrow GDL}_{Pore}$ gradients while maintaining a constant I/C ratio.[61–63] For the $TP^{\nearrow Mem}_{Particle\ Size}$ gradient, a reduced dissolution rate of the active metal from the catalyst support was observed. Long-term stability is a particularly interesting topic for future works on gradients.

Potential high-throughput fabrication techniques.—Bridging the gap from research to industrial relevance requires suitable manufacturing techniques for graded catalyst layers. These techniques should be versatile, capable of high throughput manufacturing, and able to adapt to more complex layer morphologies. Such morphologies could include the profiles shown in Fig. 6. The profiles found in the literature are smeared-out step functions (Fig. 6a), where a maximum of three graded layers was reported.[12,14–18,32,34,35,51–53,57,58,64–74] A large portion of the experimental studies used spraying techniques,[18,32,34,35,52,57,64–68] while the remainder used screen-printing, 3D-inkjet printing, sputtering, or other methods.[12,53,58,69,70,72,73] These techniques have also been reported by the industry as suitable for the manufacturing of gradients.[75–83] Based on that, the following sections give brief overviews of common coating techniques and their utility for industrial scale manufacturing of graded catalyst layers.

Inkjet printing and spray coating.—Spray coating is the coating technique used most often in the literature to manufacture gradients. It relies on depositing non-agglomerated droplets from inks to form thin films on a substrate after drying (Fig. 7a). Inkjet printing is another possible technique that utilizes low-viscosity inks, in some cases suitable for up to 0.100 Pa s.[84] An advantage of Inkjet printing is the ability to precisely print patterned structures with minimal material losses.[85]

On the other hand, spray coating is less susceptible to clogging and can cover larger surface areas faster than inkjet printing.[86] Spray coaters are more established for roll coating processes, such as in the automotive sector, the semiconductor industry, and touch panels.[85] In fact, Audi® and the US Navy have already reported using spray coating to make graded catalyst layers.[76,81] Audi® reported the manufacturing of $TP^{\nearrow Mem}_{Particle\ Size}$ gradients, while the US Navy reported the manufacturing of gradients using two different catalyst supports (Ketjenblack and Vulcan).[76,81] Also, the development of a roll-to-roll ultrasonic spray coating system for PEM fuel cells has been announced, whereas such initiatives for inkjet printing are still missing.[85,87,88]

With a single coating head, TP and IP gradients can be made with spray coating or inkjet printing. TP gradients are manufactured by consecutively depositing two different inks on a substrate. IP gradients can be made by coating the substrate partially with one ink and the rest with another ink. Thus, (smeared) stepwise gradients can be manufactured with this approach. Depositing an ink with changing composition would allow this configuration to produce continuous IP gradients, but reliably feeding an ink with non-constant composition is very difficult. Thus, multiple spraying heads or arrays of inkjet printers can simultaneously be applied to reduce manufacturing time and render the gradients more continuous, as in Fig. 7c.

Limitations in spray coating and inkjet printing for upscaling include high investment costs for multiple spray or inkjet heads and the required time and equipment for drying steps between the deposition of single layers. Further, spray coating and inkjet printing are limited in their ink compositions as they typically require low-viscosity inks to prevent nozzle clogging. Also, redissolving the previously coated layer due to thin viscosities can result in non-well-defined gradients. This potential issue also remains uninvestigated so far. Another concern is the evaporated solvent in large-scale productions. Flammable solvents require special precautions and

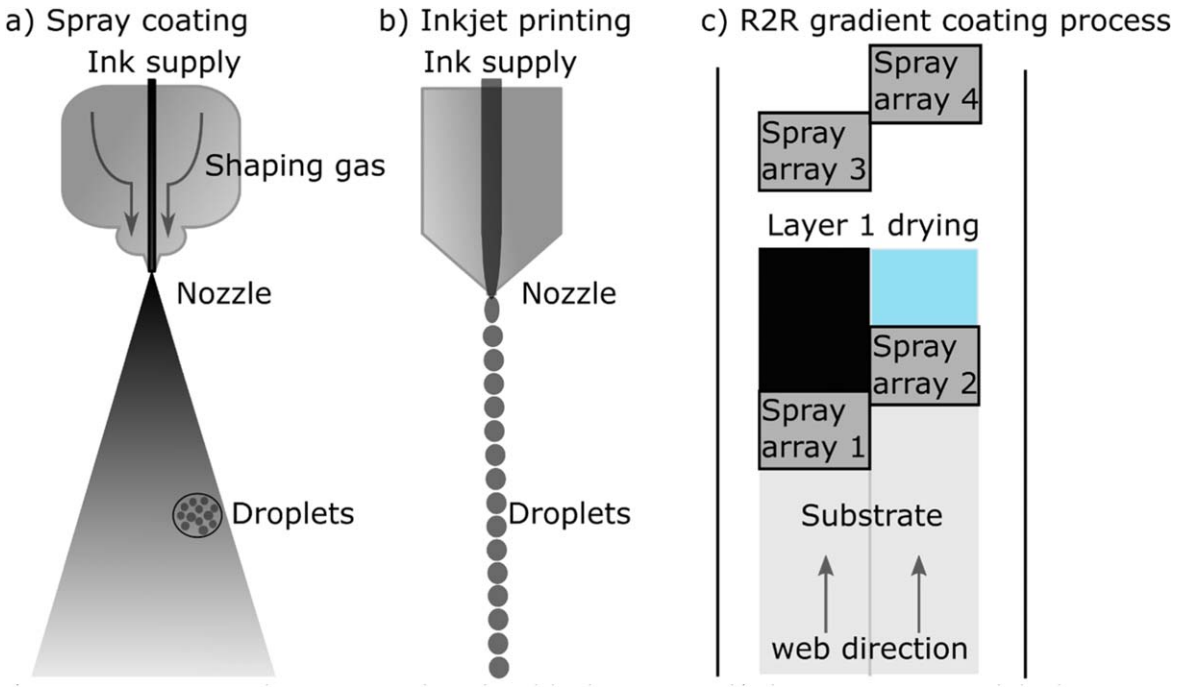

Figure 7. (a) Spray coating process with a continuous ink supply and droplet generation, (b) inkjet-printing process with droplet generation and continuous ink supply, (c) R2R coating process for IP and TP gradient fabrication using spray coating. The substrate passes under the spray arrays, where a series of coatings are applied. Pairs array 1 + 2 and arrays 3 + 4 produce IP gradients whereas arrays 1 + 3 and 2 + 4 result in TP gradients.

treatment, especially in the presence of catalysts. Furthermore, solvents with low solvent content are desired for large-scale productions due to lower operation costs. Despite the significant challenges spray coating and inkjet printing remain worth consideration due to their great versatility.[89,90]

Slot-die coating.—Slot-die coating is a pre-metered technique where the desired wet film thickness is pre-set to make the coating in one step. Compared with spray coating and inkjet printing, slot-die coaters can handle higher viscosities, up to several Pa s, at low shear rates and hundreds of mPa s at high shear rates[91] with precise adjustment of the slot-die head and other processing parameters.[92–94] Once the requirements are met, the slot-die coating becomes a compelling technique to fabricate homogenous layers quickly with dry film thicknesses ranging from 10 nanometers to several hundreds of micrometers.[94]

Alternating the design of a single slot-die coater to incorporate two slots or more enables a multilayer deposition strategy for the TP direction.[85,86,93,95,96] The coater would then be called a double slot-die coater with two slots. An illustration is provided in Fig. 8a. IP and TP gradients could theoretically be made by placing multiple double slot-die coaters in parallel. It is also possible to use single-slot die coaters to make the TP gradients with a drying step in between. The gradients would ultimately take the form of smeared out step functions.

A central concern of using double slot-die coaters is the mixing of fluids while depositing in the TP direction results into non-well-defined boundaries. This is difficult to address since the inks used often have similar properties. Single-slot die coaters in series with drying steps in between could mitigate this problem. However, such integration requires higher investment costs and more fine-tuning in optimization processes. It is also known that precisely controlling the overall loading and boundaries is challenging, especially when very low loadings are required and when the second layer is coated directly on a previously non-smooth layer.[97]

Also, the practicality of making IP gradients in both cases by placing slots in parallel is unclear. Possible artifacts include inhomogeneous film formation with thickness deviations and edge effects such as a neck-in that restricts the achievable coating width.[98] Perhaps this can be mitigated by an alternative design of the slot-die coating process. For example, 3 M™ reported the manufacturing of $IP^{\nearrow Out}_{Cat}$ gradients for enhanced current density uniformity in a fuel cell by using a die coating device which applies a thickness gradient of the wet ink across the web width, by tilting the head for example.[77] However, in this case a single ink is still used. Designs utilizing more than one ink still need to be developed. At first glance, the slot-die coating seems promising for fabricating IP and TP gradients. The utilization of low solvent inks and the high manufacturing speed makes it compelling for large scale-production. However, the suitability for gradients remains unclear, and more studies, including computational fluid mechanics models and simulations, are required.

Screen-printing.—Screen-printing is another coating technology that has been quite frequently used for electrochemical applications, like circuit boards and glucose sensors.[99–101] It is a pre-metered coating technique with good scalability from lab-scaled research to industrial relevance.[99,102] For successful coatings, high, almost paste-like viscosities are often required ranging from 0.5–50 Pa s.[103–106] Additionally, mesh designs and thicknesses must be carefully chosen to ensure a homogenous desired transfer volume.[99]

As a single ink is typically used on the screen during the deposition process, multiple screens would be needed to make TP and IP gradients. TP gradients could be made by placing multiple screens in series behind each other with drying steps in between. The IP gradients would be manufactured by placing the screens in parallel. Some manufacturers move both the frames and squeegee during the coating process to ensure a continuous roll-to-roll screen-printing process. Such a moving configuration could also be adapted. Overall, the gradients would take up the form of step functions. A

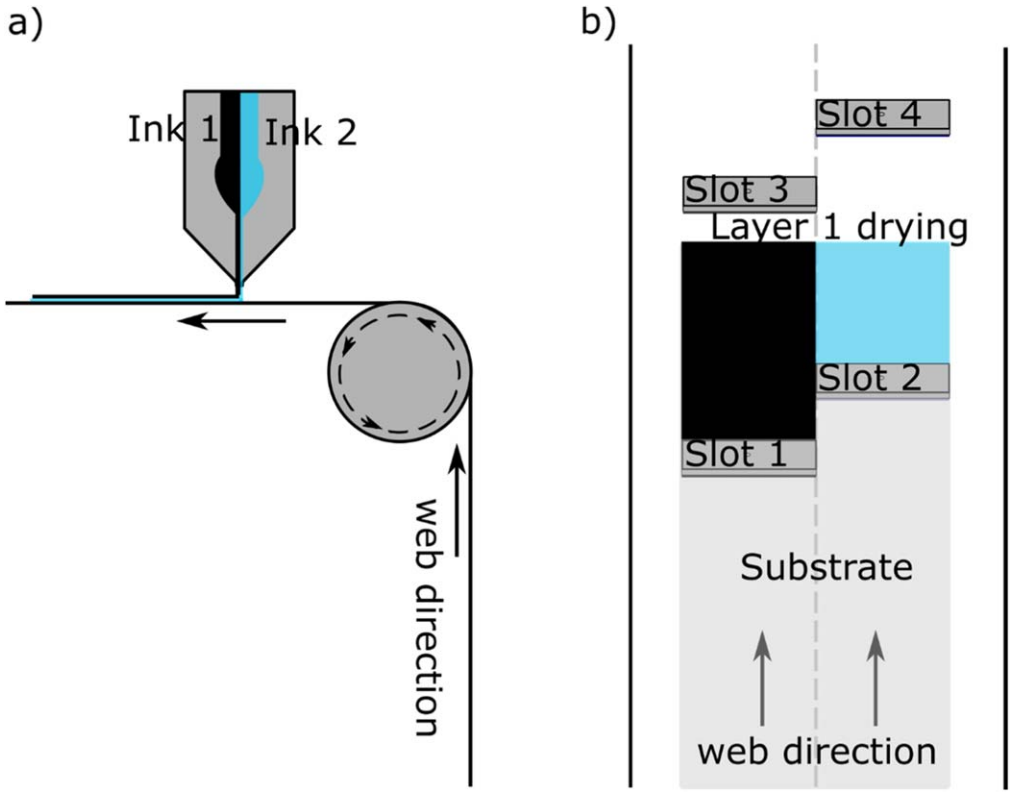

Figure 8. (a) Double slot-die coater in a roll-to-roll system for coating TP gradients. (b) R2R coating process where the substrate passes under slots 1 + 2 and then slots 3 + 4 for coating. The IP gradients are made by slot 1 + 2 and slot 3 + 4 whereas the TP gradients by slot 1 + 3 and slot 2 + 4.

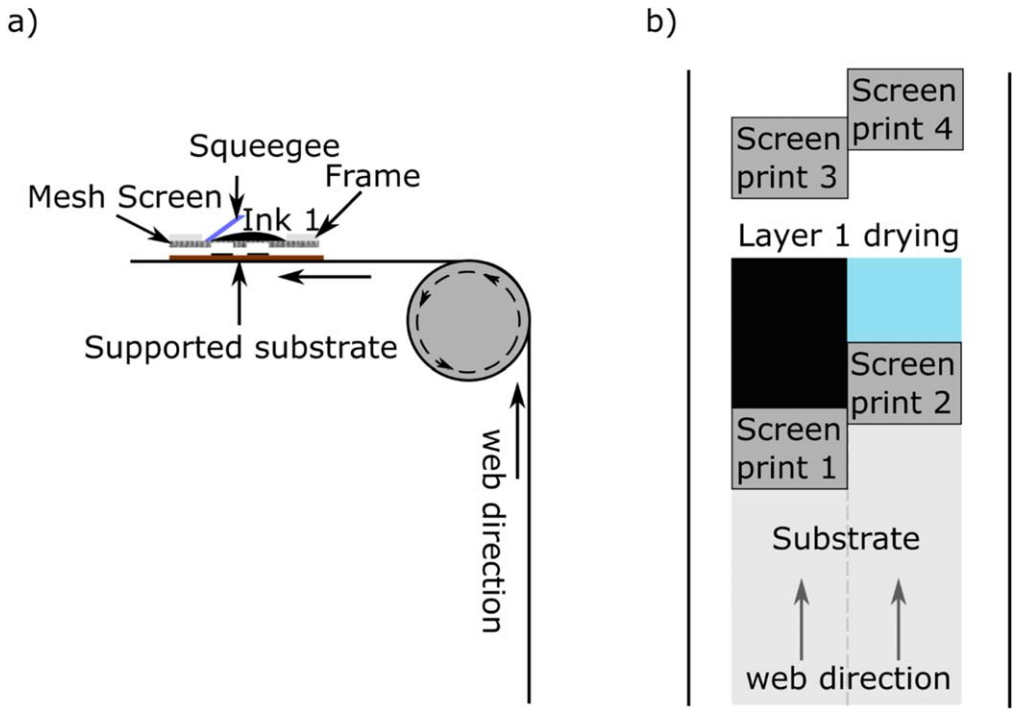

Figure 9. (a) A screen-printing process showing the pre-printing version of ink 1 on a mesh with a frame and a squeegee, (b) R2R coating process where the substrate passes under screens 1 + 2 and then screens 3 + 4 for coating. The IP gradients are made by screens 1 + 2 and screens 3 + 4 whereas the TP gradients by screens 1 + 3 and screens 2 + 4.

simplified depiction of a roll-to-roll screen-printing process to make graded catalyst layers is in Fig. 9b.

Due to the nature of screen-printing, films of different thicknesses can easily be realized with simple, cheap designs and excellent scales of economy.[99] In a matter of fact, a study by the Fraunhofer ISE reported the possibility of manufacturing in-plane gradients using screen-printing for fuel cells.[107] However, this coating technique also has some disadvantages. It requires fine-tuning for smooth coatings and also substrates with high surface quality.[103,104] The surface requirement can be problematic for TP gradients because the coated layer is not always smooth. Also, new screens are often required for process adjustments, and dry film thicknesses smaller than 5 μm can be difficult to achieve.[105]

Roll coating.—A less commonly used lab coating technique is roll coating, a collective term for coating a substrate from a rotating cylinder. It is a pre-metered coating technique whereby the roll coating involves a moving substrate and a rotating ink deposition system, the main distinguishing feature. Gravure and flexographic coating are well-known roll coating techniques with viscosity ranges from 0.05 to 0.2 Pa s depending on the shear rate.[106,108] Gravure roll coating deposits ink from cavities in the gravure roller to the substrate. As an alternative approach, flexographic printing transfers ink from a roller submerged in a bath onto a cylinder that carries ink on pads, the so-called flexographic plates. Then, the ink is transferred from the flexographic plates onto the substrate. This approach usually consumes less ink and reduces costs.[109]

Figure 10 shows a simplified flexographic printing process for making TP gradients. The substrate is first coated with ink 1 from the plate cylinder with the flexographic plates before passing to the second plate cylinder with ink 2. Patterns and thickness changes over the width of the roller can be employed to add IP gradients to the formed layers. Additionally, IP gradients could also be manufactured by placing multiple flexographic rolls parallel to each other with

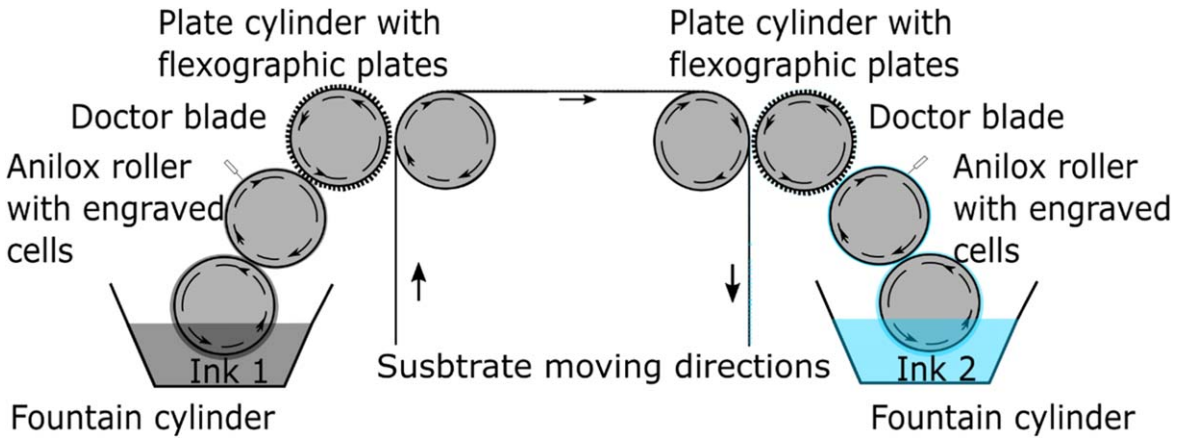

Figure 10. A simplified scheme for making TP gradients with flexographic roll coating. Ink from a submerged roller is transferred onto an anilox roll with finely engraved cells. Excess ink is removed with a doctor blade before transferring the ink onto a plate cylinder roller with flexographic plates.[111] The ink is then transferred via pressure and shearing from the plate cylinder to the impression cylinder containing the substrate.[111]

different inks similar to the previous scenarios, or more easily by patterning a single roll.[110] The gradients would then take the form of step functions.

Roll coating techniques, especially flexographic and gravure printing, are compelling for manufacturing graded catalyst layers. Their applicability in practice, though, for manufacturing gradients has yet to be investigated on a larger scale, such as in the framework of the AMO's Multi-year Program.[112] So far, only one study reported multilayers for PEMFCs using flexography printing.[113] The authors applied multiple coatings directly on a GDL to reduce crack formation with a water-based ink. The authors report the possibility of precisely controlling the platinum loading by a multilayer coating approach, but also report the presence of cracks in the final layer.[113] Such problems need to be addressed first, however, the downside of these techniques is that they are not common for lab-scale research. Also, low solvent contents are typically preferred for large scale-manufacturing. As a result, the gap between lab-scale research and industrially relevant production becomes difficult to investigate. Lab-based researchers often rely on other representative coating techniques such as bar coating, and doctor blading.

Outlook on coating techniques.—The production of graded catalyst layers on a large scale has yet to be reported. Upon closer examination, it becomes evident that design modifications and adjustments are necessary for the coating techniques. Moreover, selecting an appropriate coating technique requires a more comprehensive and detailed comparison. To facilitate this, Table I is provided, featuring relevant coating metrics scored as following: 1 = very poor; 2 = poor; 3 = Average; 4 = Good; 5 = Excellent. Ideally, each metric would be thoroughly evaluated with physical parameters and values, accompanied by detailed explanations. Additionally, it would be helpful to include electrochemical data for comparison. However, obtaining such data is not currently feasible with the available literature. Therefore, a metric scoring approach has been adopted that focuses solely on the coating technique. The chosen scores are justified, and references are provided where possible.

Ink flexibility: The viscosity significantly influences the compatibility of inks to different coating techniques. Inkjet printing typically requires colloidal systems with viscosities up to 0.100 Pa s.[84] Spray coating can accommodate higher viscosities (depending on the spray system type) and is less prone to clogging.[86] Therefore, spray coating receives a higher score than inkjet printing. Slot-die coaters can handle higher viscosities, ranging from hundreds of mPa·s at high shear rates to several Pa·s at low shear rates.[91] However, excessively high viscosities can lead to high pressure build-up in the slot-die head, resulting in poor flow behavior. Conversely, very low viscosities can cause poor wetting and ink runoff, making it challenging to achieve uniform coatings.[91,114] Consequently, slot-die coating is not very flexible for different inks and is assigned an average score three. Screen-printing requires paste-like inks with a narrow viscosity range of 0.5–50 Pa s.[103–106] Due to its limited flexibility, it receives a score similar to inkjet printing. Roll coatings, like flexography and gravure printing, have viscosity ranges from 0.05 to 0.2 Pa s depending on the shear rate.[106,108] The relatively narrow viscosity range overlaps with other coating techniques, resulting in a score similar to slot-die coating.

Minimum solvent requirement: Minimizing solvent use in inks is desirable to reduce operating costs. However, the minimum solvent required depends on the coating technique. As previously mentioned, inkjet printing often requires colloidal inks, while spray coating can handle only slightly lower solvent contents, resulting in scores of one and two, respectively.[84] Slot-die coaters typically tolerate lower solvent contents, earning a score of four, a bit better in comparison to flexography and gravure printing which we assign a score of three.[91,106,108] Screen printing requires the least amount of solvents, thus receiving the highest score.[103–106]

TP Gradients compatibility: Due to the high solvent requirements for inkjet printing and spray coating, mixing and dissolving previously coated layers by newly deposited ones is possible. This can lead to highly smeared and poorly defined gradients, depending on the overall layer thickness. Thus, despite theoretical compatibility for making TP gradients, practical challenges arise, likely necessitating high drying rates or slow spraying. Once, the challenges are addressed, spraying and inkjet-printing become compelling for TP gradient manufacturing. Roll coating also faces similar issues, but to a lesser extent due to lower solvent contents, however, precise coating control can be challenging earning it a similar score of three. Slot-die coating requires less solvent, reducing the risk of dissolving the previous layer. Different coating gaps can be used to create TP gradients earning it a score of four. For screen printing, dissolving the previous layer is minimal compared to other techniques. However, achieving the necessary surface smoothness and minimum thickness makes this technique more challenging for TP gradients earning it a score of two.[105]

IP Gradients compatibility: Inkjet printing and spray coating can be easily used to create IP gradients, as discussed in section 2.3.1. Potential artifacts such as edge effects and neck-in for slot-die coating can hinder the manufacturing of IP gradients, resulting in a lower score of two.[98] Roll coating is well-known for its ability to print patterned structures, and screen printing can also be used to create IP gradients.[107,110] Therefore, similar scores are given to roll coating and screen printing as to inkjet printing and spray coating.

Gradient shape customization: Altering the volumetric and gravimetric fractions of the single coatings in the manufactured gradients is associated with different complexity. The complexities vary depending on the coating technique and the gradient type. For example, inkjet-printers and spray coaters can include servo motors to physically move the spraying or printing head. In this way, different gradient shapes can be flexibly made for IP and TP gradients, assuming dissolving previously coated layers is not a concern. The height can be flexibly adjusted for slot-die coating to alter TP gradients, but different slot-die head designs are necessary for IP gradients, resulting in higher investment costs. Different screens are needed for both TP and IP gradients with the option of partially covering a screen-printing apparatus for IP gradients. This also involves higher investment costs. Roll coating faces similar

Table I. Comparison of different coating techniques, based on a metric scale from 1 (very poor) to 5 (Excellent).

	Inkjet-printing	Spray coating	Slot-die coating	Screen-printing	Roll coating
Ink flexibility	2	3	3	2	3
Minimum solvent requirement	1	2	4	5	3
TP Gradients compatibility	3	3	4	2	3
IP Gradients compatibility	4	4	2	4	4
Gradient shape customization	4	4	3	3	3
Coating speed and scalability	2	2	3	3	4
Ink wasted from coating	4	3	3	4	3
Applicability in lab settings	3	4	2	3	1
Innovation requirements	3	3	2	2	2

challenges leading to a similar score as slot-die coating and screen-printing.

Coating speed and scalability: Spray coating is known for its ability to cover larger areas faster than inkjet printing and is compatible with roll-to-roll systems.[85,86] It is established in the automotive sector, the semiconductor industry, and for touch panels, and has recently been in development for PEM fuel cell systems.[85,87,88] However, compared to slot-die coating, it is at least an order of magnitude slower.[115,116] Slot-die coaters can achieve web speeds of over $100\,\mathrm{m\,min^{-1}}$ and are known for their scalability.[117] The same is true for screen printing, with coating speeds above $100\,\mathrm{m\,min^{-1}}$ and holds high industrial relevance.[99,102,118] Consequently, inkjet printing and spray coating score the lowest, while slot-die coating and screen printing score higher. Roll coating techniques, such as gravure and flexographic printing, can achieve very high coating speeds of 100 to $600\,\mathrm{m\,min^{-1}}$ and are also well-known for their scalability, thus scoring the highest.[119,120]

Ink wasted from coating: Inkjet printers cause minimal material loss due to the precise deposition on the substrate from a minimal distance, with the solvent not counted as waste material.[85] Spray coaters can have considerably higher material losses due to over-spray and the greater deposition height.[121] Waste generated during screen printing is less than spray coating because of the screen and defined printing area.[122] The wasted ink usually remains on the mesh or the squeegee, so screen printing receives a higher score than spray coating. Flexographic and gravure printing can generate more waste due to the rollers and the excess ink removed by the doctor blade. This ink is not always recycled, resulting in a lower score than screen printing. Slot-die coaters can generate considerable waste at the edges that cannot be used.[123] Therefore, a lower score than screen-printing is given.

Applicability in lab settings: Spray coating is perhaps the most straightforward coating technique for labs, reflected by the number of publications available.[18,32,34,35,52,57,64–68] Screen-printing and inkjet printing are also utilized in labs due to their compactness and ease of use.[53,58,70] Slot-die coaters, on the other hand, are less commonly found in labs, and roll coatings such as gravure and flexographic printing are the least common.[77,119,124,125]

Innovation requirements: The most straightforward requirement for inkjet-printing and spray coating is increasing the coatable ink viscosity and the web speed. However, these requirements don't hinder the possibility of making IP and TP gradients. For slot-die coating, non-conventional designs are required to manufacture IP gradients precisely, whereas, for screen-printing, the surface smoothness requirement for TP gradients needs to be addressed. For roll coating, the capability to manufacture both TP and IP gradients still needs to be verified.

Techniques to determine gradients.—The cycling between manufacturing and characterization is invaluable to optimize a product. The same holds for producing gradients in catalyst layers for electrochemical cells. However, detecting minute concentration differences in mico- and nanometer-scale structures is inherently tricky. The most straightforward characterization approach is the electrochemical testing of a cell with a graded layer and the comparison with a standard reference cell. Yet, this procedure does not provide insight into the actual structure of the graded layer and if the gradient was produced as intended. Consequently, alternative techniques are sought that can provide more information, e.g., on the local chemical composition or the morphology of the catalyst layer.

A first differentiation has to be made between IP and TP gradients: IP gradients are found on the millimeter-scale, while TP gradients are on the small micrometer-scale. Thus, different methods are suited for characterizing the two kinds of graded catalyst layers. To date, reports in the literature on the characterization of gradients are only scarcely available. Therefore, this section provides an overview of techniques likely suited to perform such an analysis rather than summarizing studies that performed the evaluations.

Due to their larger accessible surface area, IP gradients are inherently easier to characterize than TP gradients. For example, a difference in catalyst loading along the area of a catalyst layer can be measured using physicochemical approaches such as thermogravimetric analysis or inductively-coupled plasma mass spectroscopy (ICP-MS) to quantify the metal content of a sample.[126–129] For this analysis, the samples must be cut according to the gradient and measured separately to identify systematic differences between the sample areas. Similarly, this sample preparation can be employed to perform porosimetry or physisorption measurements to detect changes in the surface area along the area of a catalyst layer. For instance, Lobato et al. employed Mercury intrusion porosimetry to evaluate the influence of the Pt/C-ratio in the catalyst layer on characteristics like pore size distribution and porosity, which shows that this method has the potential to detect IP gradients.[130] Furthermore, a characterization with X-ray photoelectron spectroscopy can be used to measure the elemental composition on the surface of a sample considering a statistical analysis approach due to high sensitivity of this technique. For example, this method was applied to the catalyst layer of a direct methanol fuel cell and revealed a loss in catalyst loading during operation.[131] Thus, this approach harbors the potential to detect and quantify IP gradients in catalyst layers.

IP gradients can also be detected via microscopic approaches. Depending on the method and the gradient type, a morphological or compositional gradient can be measured. Differences in surface morphology can be detected with various instruments, like optical microscopes, confocal laser scanning microscopes, profilometers, scanning electron microscopes, and atomic force microscopes.[132,133] Depending on the microscopic technique's spatial resolution, different surface morphology features, like cracks, grains, or pores, can be resolved. Differences in the three-dimensional structure in IP direction can be quantified with advanced imaging techniques, like high-resolution computed tomography, focused ion beam scanning electron microscopies tomography (FIB-SEMt), and transmission electron microscopy tomography (TEMt). Elemental analysis of IP gradients can also be combined with some imaging techniques. For example, X-ray fluorescence (XRF) (resolution 5μm) or energy-dispersive X-ray spectroscopy (EDX) can be used.[134] Among these techniques, XRF microscopy has been successfully used to qualitatively determine the loading of catalyst layers.[135,136] The downside of the microscopic and elemental approaches is that these measurements can be time-consuming and typically only evaluate small fields of view, which render them unsuited for routine analyses of heterogeneous samples. However, in some cases integrating microscopic or spectroscopic techniques directly in-line is relevant, making these very interesting and promising candidates for future gradient manufacturing.

TP gradients need to be analyzed using high-resolution approaches due to the small length scale. Also, more elaborate sample preparation techniques are required to access the features of interest. The most straightforward approach is a physical cross-section prepared by cryo-fracturing the sample or by embedding the sample into a matrix (like epoxy resin) that enables the sample to be grinded and polished to reveal a high-quality cross-section of the graded catalyst layer. Next, the sample can be investigated using SEM and EDX. However, depending on the catalyst layer thickness and the type of gradient, the resolution capabilities of SEM may not be sufficient to measure a gradient in a TP direction. For instance, Kim et al. created MEAs with a TP gradient in ionomer binder content and performed SEM imaging on cross-sections but could not identify differences between the different gradient configurations.[13] Also, catalyst layers can be thinner than $10\,\mu\mathrm{m}$, and the layers are highly porous (porosities of 50% or more), which means that a single cross-section may not be representative of the whole sample.[137] The latter issue can be tackled by performing 3D imaging on a sufficiently

large area using FIB-SEM. With this approach, a 3D image of the sample is created by subsequently removing the surface of the sample by milling with an ion beam, followed by imaging using SEM.[137] Another approach to 3D imaging is computed tomography, which employs X-rays and detects differences in beam attenuation (absorption) or phase contrast. Nano-CT is available with a resolution of up to several nanometers. This method has been employed to detect, e.g., differences in pore size distributions within catalyst layer samples of different ionomer contents which hints toward its possible application in graded samples.[138] Nonetheless, these approaches may fail when catalyst layers are thin or when gradients in materials with poor contrast, such as polymeric binder versus carbon support, need to be characterized.

TEM or scanning probe microscopy are possible techniques to identify TP gradients in such cases. Scanning probe microscopy, such as atomic force microscopy, measures the interaction between the sample surface and a nanometer-sized probe, providing information on sample topography and, e.g., adhesion characteristics. With this technique, the ionomer content of a standard electrode of a PEMFC was measured, and a slight gradient was detected.[139] The sample preparation for this imaging method relies on producing high-quality cross sections, which is, e.g., possible using ion milling or physical sectioning using ultramicrotomy. The latter method can also prepare samples for TEM by cutting ultra-thin (<200 nm) sections from a sample. TEM outperforms SEM in terms of resolution, and it also harbors the option to employ EDX for an elemental analysis on the nanometer-scale. For instance, TEM has been employed to qualitatively evaluate an ionomer gradient in a PEMFC electrode.[32]

Conclusions

Catalyst layers inherently have inhomogeneous protonic conduction profiles and concentration profiles for the reactants, products, and charge carriers in the IP and TP directions. Graded catalyst layers can compensate for the inhomogeneity and, in some cases, reduce costs, increase power densities, and extend the durability of the MEA. Existing studies show that grading catalyst layers is a powerful technique to improve performance benchmarks in PEMFC systems, yet many open questions remain. For example, which gradients are the most effective and straightforward to manufacture on a large scale from an industrial perspective? Is it possible to simultaneously reduce the costs, increase power density, and extend the durability of an MEA using the same gradient type? Or can multiple gradients be easily combined, for example $TP^{\nearrow Mem}_{Ion}$•$TP^{\nearrow Mem}_{Pt\ particle\ size}$ gradients, for better performance and durability? Is it possible to achieve a continuous $TP^{\nearrow Mem}_{Ion}$ gradient without coating multiple catalyst layers? If so, what would then be the advantages of multiple coated layers?

From the conducted literature review, we notice that many simulations remain to be experimentally proven, and that the presence of gradients in experiments isn't always verified. We also notice discrepancies for the optimal through-plane catalyst distribution. Additionally, many promising gradient types remain uninvestigated as mentioned in the summary. Furthermore, studies involving combinations of gradient types such as $TP^{\nearrow Mem}_{Ion}$•$TP^{\nearrow GDL}_{PTFE}$•$IP^{\nearrow Out}_{Cat}$ gradients are still missing. These are important to investigate at an early stage, as different gradients can optimize different processes, and suitable coating techniques designs could differ depending on the intended gradients for manufacturing.

Investigations of multiple gradient types can be challenging and time-consuming due to difficulties with manufacturing and characterization. However it is important to do so at an early research level, before an economy of scale effect. Also before scaling up the production of fuel cell cells, the realization of optimized gradients in real applications requires tackling two notable challenges that were discussed in this study: first, the development and implementation of suitable manufacturing techniques, and second, the imaging and characterization of the gradients themselves. For manufacturing, we notice that the most straightforward method to make gradients is via spray coating or inkjet printing. However, slow production speeds, high CAPEX and OPEX costs, and increased safety concerns make such methods not favorable for large scale-production. This is not the scenario for roll-coating, slot-die coating, and screen-printing. Screen-printing and slot-die coating are likely more attractive than roll-coating due to less solvent requirement and thus lower operating costs. Furthermore, these two techniques are well-established industrially for large scale-production and can be easily scaled up from the lab. However, their compatibility for gradient manufacturing is associated with some challenges. As discussed, low Pt-loaded TP gradients can be problematic for screen-printing. For slot-die coating, thickness deviations at the edges can pose as an obstacle for IP gradients. However, as mentioned, this can vary depending on the intended gradient type for manufacturing. For example, an $IP^{\nearrow Out}_{Cat}$ gradient can be made using slot-die coating by tilting the slot-die head, which would result in varying wet film thicknesses. However, an IP gradient with two different inks cannot be made as easily. To overcome these challenges, further research and possibly new designs are required for the manufacturing of graded catalyst layers on large scales.

For the characterization of gradients, one notices that the complexity of characterization differs between IP and TP gradients. Since IP gradients are found on the millimeter-scale, they can be detected more readily than TP gradients. However, the techniques suitable for TP gradients can also be utilized for IP gradients. Among the methods that can be used to characterize both gradient types are physically cutting and cross-sectionally preparing electrodes for SEM-EDX or TEM-EDX, and performing 3D reconstruction using FIB-S/TEM or using Nano-CT.

Overall, grading catalyst layers is a powerful optimization technique to enhance fuel cell performance, reduce costs, and increase durability. By developing and employing suitable coating techniques and thorough characterization, graded catalyst layers have the potential to be precisely engineered for optimal functionality. Ultimately, graded catalyst layers could be the fuel cell of tomorrow.

Acknowledgments

We gratefully acknowledge the financial support provided in the frame of the POREForm project funded by the German Federal Ministry for Economic Affairs and Climate Protection (BMWK; funding number 03ETB027A).

Appendix

Table A·1. Summarizing table of investigated gradients for PEMFCs.

Specifications	Study and Results
-Antoine et al.[140] -TP catalyst gradient -numerical + experimental -drop casting on RDE	The study was conducted in an RDE with a Nafion™ membrane at the electrolyte interface with 1 M of H_2SO_4. The RDE had a fixed temperature of 293 K, and O_2 was used for the ORR. Vulcan-based catalysts (Pt/C 20% and 30%) were mixed with pure Vulcan carbon while keeping the total Pt loading the same among different samples. A volumetric Nafion™/carbon ratio of 1 was chosen for the non-porous samples, whereas porous samples had volumetric fractions of 0.3, 0.2, and 0.5 for carbon, PTFE®, and Nafion™, respectively. By drop casting different compositions and inks, Pt gradients were made. From RDE measurements, the authors saw that diffusion and ionic ohmic drop limitations are still relevant in the kinetic regime, resulting for non-porous layers, a preferential catalyst distribution close to the GDL and for porous layers, a preferential catalyst distribution close to the membrane.
-Yoon et al.[34] -TP ionomer gradient -Experimental -spraying	Sprayed a 40% Pt/C catalyst with Nafion™ contents varying between 10 wt% and 60 wt% to make DCLs. The DCLs had equal Pt loadings among the layers of ∼0.2 mg cm^{-2}, and the samples were tested at 60 °C, over-humidified conditions, ambient pressure, in H_2-O_2, and H_2-air. A 35 wt% Nafion™ layer coated on top of a catalyst layer outperformed DCLs with ionomer weight content gradients from 10% to 60% (increasing and decreasing to the membrane), with the maximum current being around 1.2 A cm^{-2}.
-Wilkinson et al.[141] -IP gradients -numerical+experimental	Studied in-plane stress gradients including temperature, oxygen, and pressure gradients through experiments and simulations from conservation equations such as mass balances. Experimental tests were done at 80 °C, 100% RH, and 3 bars with H_2-air. With pierced carbon paper, grooved ones, and varying Pt loading distributions between the inlets and outlets, the authors proposed in-plane catalyst loading and GDL pore size gradients to reduce stress factors.
-Wang et al.[31] -TP ionomer gradients -numerical	Developed a macro-homogeneous model with increasing ionomer gradients towards the membrane, where the cathode CL was assumed to consist of a matrix of carbon, platinum, and an ionomer with homogeneously distributed pore space. The cathode CL consisted of 20 wt% Pt/C catalyst with a total Pt loading of 0.42 mg cm^{-2} and the model assumed a fixed proton conduction value of 0.07 S cm^{-1}. The authors found an optimum ionomer content of 35 wt% for a single catalyst layer. Grading three CLs with ionomer contents of 30 wt%, 35 wt%, and 40 wt% increasing towards the membrane resulted in improved performances. An opposite gradient resulted in a worse performance.
-Xie et al.[32] -TP ionomer gradients -numerical + experimental -spraying	Confirmed experimentally the numerical results from Wang et al.[31] by spraying two uniform samples (Pt/C 20 wt%, Pt Loading ∼0.52 mg cm^{-2}) with Nafion™ contents of 30 wt%, 40 wt%, and two graded TCLs, $TP_{Ion}^{\nearrow \frac{Mem}{GDL}}$, with layers containing 20 wt%, 30 wt%, and 40 wt% of Nafion™ (equal Pt Loadings of 0.17 mg cm^{-2}). The samples were tested at 75 °C, 101,325 kPa, and over-humidified conditions with H_2 and O_2. The highest current density was for a $TP_{Ion}^{\nearrow Mem}$ gradient reaching ∼ 2 A cm^{-2} at ∼ 0.3 V (550 mg cm^{-2}), followed by a uniform sample 30 wt% reaching ∼ 1.7 A cm^{-2} at 0.3 V (460 mW cm^{-2}). No considerable differences were visible at 0.6 V.
-Song et al.[39]- -TP catalyst and ionomer gradients -numerical	The PEMFC performance was optimized via Pt and ionomer gradients in the through-plane direction by single variable optimizations. A Pt single variable optimization with a fixed ionomer content of 30 wt% showed a linearly increasing catalyst gradient towards the membrane as beneficial for different Pt loadings. A single variable optimization study for the ionomer content (fixed Pt loading of ∼0.52 mg cm^{-2}, 20% Pt/C) linearly increasing the ionomer content from 20 wt%–30 wt%,–40 wt% results in better performances than a uniform sample with 30 wt%. A minor improvement was achieved when the ionomer content increased linearly from 21 wt% near the GDL to 46 wt% near the membrane interface. However, a two-variable optimization for the Pt loading and ionomer content showed an increasing convex function as the optimum.
-Zhang et al.[51] -TP ionomer and binder gradients -experimental -spraying and a wet method	Made DCLs consisting of Nafion™ and PTFE binders (40 wt% Pt/C, total Pt loading ∼0.3 mg cm^{-2}). The PTFE-bonded CL has 30 wt% of PTFE in the CL, and 30 wt% of the total weight, of Nafion™ ionomer dispersion sprayed on top. The Nafion™ -bonded CL had 30 wt% of ionomer in the CL. The dual-bonded catalyst layer had equally Pt-loaded CLs (0.15 mg cm^{-2}) with once 30 wt% PTFE and 46 wt% Nafion™ ionomer on top. The samples were tested at ambient pressure, 60 °C and over humidified reactant gas at 65 °C, with once H_2-air, and once H_2-O_2 The dual-bonded CL resulted in ∼50% improvement (676 mW cm^{-2}) in peak power density compared to the PTFE-bonded cathode (452 mW cm^{-2}) and ∼28 % improvement compared to the Nafion™ -bonded sample (530 mW cm^{-2}) in O_2. In air a maximum power density of ∼250 mW cm^{-2} was for the dual-bonded CL.
-Wan et al.[69] -TP catalyst gradients -experimental -screen printing and sputtering	First screen-printed ink on GDL, followed by Pt sputtering for the anode electrode. Surface was then impregnated with ionomer before being sputtered again. Processes was repeated until three sputtered layers were achieved. The samples were tested at 25 °C, 40 °C, and 65 °C at ambient pressures and 100 kPa backpressure, using H_2-O_2. Three sputtered multilayers result in improved performances, compared to a single sputtered layer for the anode with a loading of ∼0.1 mg cm^{-2}, however, the maximum current density for samples was below 1 A cm^{-2}.

Table A·1. (Continued).

Specifications	Study and Results
-Santis et al.[56] -IP catalyst gradients -experimental	Current density distribution measurements were done at 70 °C in a fully humidified H_2-air atmosphere at 2 bars with average Pt loadings of 0.6 mg cm^{-2}, for a 205 cm^2 semi-segmented cell (8 segments) at currents of 195 mA cm^{-2}, 390 mA cm^{-2} and 585 mA cm^{-2}. Pt/C ratios of 10 wt%, 20 wt%, 30 wt%, and 40 wt% were used for that, and the ionomer loading was 0.6 mg cm^{-2}. Current density can be homogenized by in-plane Pt gradients via increased Pt loadings towards the air channels/outlet. Current homogenization won't necessarily result in better performance but likely positively affect the lifetime.
-Taylor et al.[70] -TP catalyst gradient -experimental -inkjet printing	Increasing the Pt/C wt% content from the GDL towards the membrane from 10: 20: 50 and the Nafion™ content from 20 wt% to 40 wt% improves the performance compared to a single catalyst layer (SCL) with an ionomer content of 30 wt% and a 20 wt% Pt/C catalyst. The peak power density improved from ∼320 mW cm^{-2} to ∼390 mW cm^{-2}. The graded electrode was most likely the anode. The total Pt loadings were 0.52 mg cm^{-2}, and the samples were tested at 80 °C at 100% RH in H_2-O_2.
-Prasanna et al.[57] -IP catalyst gradient -experimental -spraying	Increasing the cathode catalyst loading towards the outlet while keeping the overall loading the same results in an improved performance compared to a single coated layer at 80 °C and supersaturated conditions. The gradient (with Pt/C 40 wt%) increased towards the outlet from 0.2 mg cm^{-2} to 0.35 mg cm^{-2} with a total Pt loading of 0.3 mg cm^{-2}. Compared to homogenous catalyst layer with 0.3 mg cm^{-2}, the power density improved from 504 mW cm^{-2} to 590 mW cm^{-2}.
-Kim et al.[13] -TP catalyst and ionomer gradients -experimental -membrane coating and spraying	Made DCLs with various ionomer and catalyst distributions. The sublayer close to the membrane had a Nafion™ content of 33 wt% and 0.12 mg $cm^{-2}$of Pt (45 wt% Pt/C ratio) for all MEAs. The sublayer close to the GDL had 0.28 mg cm^{-2} of Pt and lower Nafion™ contents of 26.5 wt%, 23 wt%, 16.5 wt%, and 10 wt%. The overall Pt loading in the 5 × 5 cm^2 cell was 0.4 mg cm^{-2} and the samples were tested at a relative humidity of 95±3%, at 80 °C. The DCL with Nafion™ contents of 26.5 wt% and 23 wt% in the second sub-layer close to the GDL showed better performances than the pristine MEA (with 33 wt% Ionomer) in the high current density regime (respectively ∼0.35 V, ∼0.38 V, and ∼0.28 at 1.6 A cm^{-2}). The peak power density improved therewith by ∼25 to 30%. Increasing the catalyst and ionomer weight content towards the membrane while keeping the overall same loading results in improved performances
-Jain et al.[40] -TP catalyst gradients -numerical	An agglomerate model was used to investigate the Pt catalyst distribution. Minimum Pt loading should increase to reach the same current density at higher voltages. Maximizing the current density at a certain voltage, results in an exponential decay of Pt loading (scenario with total Pt loading of 0.1 mg cm^{-2}) from the membrane interface. (maximum loading) towards the GDL interface (minimum).
-Srinivasarao et al.[45] -TP catalyst and ionomer gradients -numerical	A spherical two-dimensional agglomerate model was used to study graded CLs in the through-plane direction for the cathode side. The two-dimensional two-phase model considered the transport of the reactant gases O_2, N_2, and $H_2O_{(v)}$, and liquid osmotic-and-diffusion water transport in the membrane. The model was validated with experimental data with a Pt cathode loading of 0.4 mg cm^{-2} operated at 70 °C, 2 atm, and 100% RH with H_2-air. Increasing the ionomer weight fraction (four CLs) with ionomer contents from 22 wt% to 34 wt% and catalyst distribution from 0.08 mg cm^{-2} to 0.12 mg cm^{-2}, towards the membrane results in improved performances compared to CLs having ionomer contents of 22 wt% and 34 wt%.
-Su et al.[43] -TP catalyst and ionomer gradients -experimental -spraying	Made DCLs with different catalyst distributions and catalyst layer thicknesses (Pt/C of 40 wt% and 10 wt%). For both cathodes and anodes the overall Pt loadings were 0.12 mg cm^{-2} and 0.04 mg cm^{-2}. respectively. The ionomer content close to the membrane was fixed at 33 wt%, and close to the GDL at 20 wt%. The cells were tested at 60 °C cell temperature at fully humidified conditions, with H_2-air applying a backpressure of ∼1.3 bar. The best performance was achieved for a DCL with equal CL thicknesses, and higher Pt distribution close to the membrane (80% close to the membrane). The power density, compared with a single coated catalyst layer with 33 wt% ionomer content, improved from ∼580 to 660 mW cm^{-2}.
-Su et al.[64] -TP catalyst and ionomer gradients -experimental -spraying	Made DCLs with a Nafion™ content of 33 wt% in the inner layer (close to membrane) and 20 wt% in the outer layer (close to GDL) and varied the Pt distribution and catalyst layer thicknesses using Pt/C catalysts of 40 wt % and 10 wt%. The Pt loading for the cathodes was 0.2 mg cm^{-2}. The samples were tested at 65 °C at fully humidified conditions and ambient pressure with H_2-air. Compared to a uniform single catalyst layer with 33 wt% of a ionomer content, a Pt distribution of 8:2 (inner:outer) with equal layer thicknesses resulted in the best performance, from ∼540 mW cm^{-2} to ∼720 mW cm^{-2}.
-Matsuda et al.[71] -TP catalyst gradients -numerical + experimental	Experimentally, the authors used ketjenblack-based catalyst supports, TEC10E30E (28.2% Pt/C) and TEC10E50E (45.7% Pt/C) with ionomer/carbon ratios of 0.78 and measured DCLs at 80 °C. Two DCLs were compared with once more catalyst at the membrane interface (∼0.25 mg cm^{-2}) and less catalyst at the GDL interface (0.10 mg cm^{-2}). In pure H_2-O_2 and at RHs of 60% and 30%, more catalyst at the membrane interface showed better performances in the IR-free polarization curves. At 90% RH, no differences were visible with pure O_2. By decreasing the O_2 concentration to 10%, more catalyst close to the GDL interface resulted in slight improvements in the IR-free polarization curve. Volumetric catalyst concentration should be highest close to the membrane interface at low RHs, and highest close to the cathode GDL at high RHs.

Table A·1. (Continued).

Specifications	Study and Results
-Srinivasarao et al.[44] -TP catalyst and ionomer gradients -numerical	A spherical two-dimensional agglomerate model was used to study graded CLs in the through-plane direction for the cathode side. The two-dimensional two-phase model considered the transport of the reactant gases O_2, N_2, and $H_2O_{(v)}$, and liquid osmotic-and-diffusion water transport in the membrane. The mode was used to maximize the current density for a given voltage for fixed Pt-loadings of 0.4 mg cm^{-2} and 1 mg cm^{-2} using four catalyst layers. For optimized performances, the void fraction always decreases from the CL/GDL interface towards the CL/membrane interface. The ionomer weight fraction should increase from the GDL to the membrane. At high current density, the Pt loading starts decreasing from the GDL to the membrane. The gradient size and weight fractions change depending on the operating voltage for all gradients.
-Jung et al.[65] -TP catalyst and ionomer gradients -experimental -spraying	Made DCLs with a total Pt-loading of 0.4 mg cm^{-2} and inner Nafion™ contents (close to membrane) of 30 wt% and outer Nafion™ contents (GDL side) of 25 wt% for both anodes and cathodes using self-synthesized Pt on carbon nanotubes with Pt/CNT ratio of ∼34 wt% and commercial 46 wt% Pt/C catalyst. The commercial Pt/C catalyst was used at the GDL interface for all samples. The samples were tested at 100% RH at 65 °C and ambient pressure with H_2-air. Placing 0.2 mg cm^{-2} of Pt/CNT close to the membrane interface resulted in a power density improvement from ∼430 mW cm^{-2} to ∼580 mW cm^{-2} compared to a homogenous Pt/C electrode with ionomer content of 25 wt%.
-Roshandel et al.[42] -TP and IP catalyst gradients -numerical	Used an agglomerate model verified with experimental data from another study to investigate the effects of oxygen concentration and catalyst distribution on cell performance. Increasing catalyst loading under the channel and to the membrane improves the performance compared to a pristine CL, due to higher local reaction rates at cell temperature of ∼70 °C, 3 atm, with H_2-air. The total Pt loading for the study was assumed constant and the power density improved by 7% for a uniform Pt loading.
-Qiu et al.[53] -TP catalyst and binder gradients -experimental -screen printing and spraying	Made DCLs for the cathode with the outer layer (close to GDL) consisting of electrocatalysts on two different carbon supports (Ketjen Black and Vulcan, 3:7 wt%:wt%) with a hydrophobic binder (PTFE). The inner layer (close to membrane) only had ketjebnlack as a catalyst support and a hydrophilic Nafion™ binder (1:1, Pt/C: Nafion™). A DCL with a total cathode loading of 0.28 mg cm^{-2} outperformed a single coated cathode layer with a loading of 0.70 mg cm^{-2} when tested at 75 °C, 0.2 MPa backpressure, and a RH of 80% in H_2-air. The power densities were improved from ∼720 mW cm^{-2} to ∼ 760 mW cm^{-2}
-Fofana et al.[72] -TP Pt gradients -experimental -sputtering on coated carbon- Nafion™ layers	Made cathode multilayers by alternatively sputtering Pt (overall loading 0.05 mg cm^{-2}) and coating carbon-Nafion™ layers with ratios of 1:2.5. The samples were tested at 80 °C and 80% RH using H_2-air gases and compared to standards having Pt loadings of ∼0.2 mg cm^{-2} where one of the standards didn't include an MPL for the GDL (peak power density ∼380 mW cm^{-2}). The multilayers outperformed a single sputtered CL, having overall the same Pt loading (from ∼330 mW cm^{-2} to ∼580 mW cm^{-2}). The standard sample with an MPL displayed the highest power density of ∼590 mW cm^{-2}, whereas the maximum power density among the graded samples was ∼580 mW cm^{-2} for a three-layered sample.
-Zhao et al.[50] -TP binder gradients -experimental -spraying	Compared conventional electrodes with DCLs having an outer PTFE bonded catalyst layer close to the GDL (40% Pt/C in 60 wt% PTFE solution) and an inner ionomer bonded catalyst layer at the membrane interface (catalyst to Nafion weight ratio of 3:1). The overall Pt loading was fixed to ∼0.4 mg cm^{-2}. The samples were tested at 50°C under ambient pressure at fully humidified conditions with H_2-O_2. Distributing 25% of the catalyst in the PTFE outer layer for the cathode can improve the performance at high current densities from ∼720 mW cm^{-2} to ∼800 mW cm^{-2} compared to a conventional electrode without PTFE.
-Cetinbas et al.[41] -TP and IP catalyst and ionomer gradients -numerical	Used an agglomerate model to study the influence of the catalyst distribution on fuel cell performance while fixing the total Pt loading to 0.3 mg cm^{-2} and the ionomer weight fraction to 30%. The study was done at 80 °C, 2 atm, and a relative humidity of 70%. Higher Nafion™ content towards the membrane interface (40_30_20%) improved the performance from ∼430 mW cm^{-2} to ∼470 mW cm^{-2}. Higher catalyst loading towards the membrane interface (m(Pt):0.35_0.30_0.25 mg cm^{-2}) improved the cell performances compared to a single CL from ∼430 mW cm^{-2} to ∼450 mW cm^{-2}. A higher Nafion™ content and catalyst loading under channel improved the performance at high current densities by similar amounts.
-Kim et al.[73] -TP catalyst gradients -experimental -decal transfer and GDE coating	Made DCLs with different Pt catalyst distributions while fixing the total Pt loading to ∼0.4 mg cm^{-2} using a commercial 45.8 wt% Pt/C catalyst. The ionomer content was 25 wt% for all samples. The DCLs were made by directly coating different Pt loadings on the GDL and the remaining Pt via a decal transfer process. The samples were tested at 65 °C at 100% RH in H_2-air. Compared to a single CL (Decal transferred), a higher Pt distribution in the layer closer to the membrane (∼0.3 mg cm^{-2}) and a lower one close to the GDL (∼0.1 mg cm^{-2}) results in improved performances (0.142 V vs 0.293 V at 1.6 A cm^{-2}). However, the peak power densities improved only slightly from ∼580 mW cm^{-2} to ∼610 mW cm^{-2}. Coating completely on the GDL resulted in the worst performance due to the intrusion of the catalyst ink into the GDL (max power density ∼260 mW cm^{-2}).

Table A·1. (Continued).

Specifications	Study and Results
-Xiong et al.[52] -TP binder gradients -experimental -air brushing	Made cathode DCLs with a hydrophobic outer layer (PTFE) and a hydrophilic inner layer (Nafion™) for air-breathing PEMFCs. The inner layer had 30 wt% ionomer content and the outer layer a mixture of 10 wt% PTFE and 20 wt% ionomer, while the total Pt loading for all samples was 0.3 mg cm^{-2} (47 wt% Pt/C). The samples were tested in H_2-air at a room temperature of 26 °C. The DCL with PTFE displayed slight improved performances (∼160 mW cm^{-2}) compared to the SCL (∼140 mW cm^{-2}) with PTFE.
-Zhang et al.[58] -IP catalyst gradients -numerical + experimental -screen printing	Performed current density distribution measurements using MEAs with three segments of different catalyst loadings, increasing towards the outlet at 80 °C and 3 atm. A gradient increasing from 0.2 mg cm^{-2}, 0.31 mg cm^{-2}, and 0.42 mg cm^{-2} to the outlet was compared to a uniform cathode loading of 0.3 mg cm^{-2}. The overall performances were overlapping, slightly better for the uniform catalyst layer. However, the gradient showed 31% higher degree of current uniformity. The authors concluded that in-plane gradients can mitigate aging by preventing hot spots because of a homogeneous current distribution. The optimal catalyst distribution was also found to be a function of the operating voltage and current.
-Ebrahimi et al.[142] -TP and IP catalyst gradients -numerical	Used a numerical model at ∼73 °C, 3 atm, and with H_2-air to find an optimal distribution for the catalyst loading. The authors observed that the oxygen concentration is the highest under the channel and decreases under the land and in the through-plane direction towards the membrane. Increasing the catalyst content along the channel increased the performance by ∼7%. Additionally, homogenizing the current density distribution would not necessarily result in a better performance.
-Ye et al.[74] TP catalyst gradients -experimental -membrane filtering technique	Manufactured DCLs with an increasing catalyst loading and decreasing pore size towards the membrane. A commercial 20% Pt/C catalyst was used in combination with carbon nanotubes (10–15 nm in diameter) and carbon nanofibers (100–200 nm in diameter and 30–100 μm in length) to make a Pt rich layer at the membrane interface and a Pt poor layer at the GDL interface, with a total Pt loading of 0.09 mg cm^{-2} for the cathode. The anode was a single layer with a total Pt loading of 0.2 mg cm^{-2}. For the cathode, a Nafion™ solution was sprayed on top to achieve a total ionomer loading 0.285 mg cm^{-2}, which is identical to a total I/C ratio of ∼0.7. The DCL was compared with a sample having single layered catalyst layers at 100% RH in H_2-air and found to result in ∼11% peak power density improvement which was explained with better transport properties (from ∼428 mW cm^{-2} to ∼475 mW cm^{-2}).
-Herden et al.[59] -IP ionomer equivalent weights gradients -experimental -decal transfer	Made an in-plane ionomer equivalent weight graded MEA, with an increasing EW towards the outlet. The anode loading was 0.08 mg cm^{-2} and the cathode 0.3 mg cm^{-2} while the I/C ratios was fixed at 0.8, and the EWs were 772 and 825 $g_{polymer}$ $mol^{-1}_{SO_3^{-1}}$. The MEAs were tested in H_2-air with a dew point of 55 °C while changing the cell temperature between 55°C and 80 °C to result in RHs from 33% to 100%. Compared with cathodes having only one EW, the graded MEA with low and high EWs resulted in improved performances in the high current density regime and a larger flexible operating range with regards to the relative humidity when compared to electrodes with uniform EWs.
-Ebrahimi et al.[143] -TP and IP catalyst gradients -numerical	Investigated the influence of the catalyst distribution along the channel using a multiphase mixture model with two-phase transport mechanisms while keeping a fixed Pt loading. The model was verified with experimental data from another study. The humidified inlet cathode flow temperature was set at 80 °C and the backpressure to 0.3 MPa. Increasing the catalyst loading up to a certain amount at the channel entrance and where the reaction rate is the highest results in improved performances by 14%.
-Xing et al.[30] -TP catalyst and ionomer gradients -numerical	Used an agglomerate model with two-phase flow mechanisms to investigate linearly decreasing catalyst and linearly increasing ionomer loadings from the CL/GDL interface towards the CL/membrane interface of the cathode electrode at 70 °C, 0.1 MPa, 100% RH, in H_2-air. The total Pt loading was between ∼0.2 and 0.8 mg cm^{-2} (40% Pt/C), and the ionomer loading between 0.9 mg cm^{-2} and 1.65 mg cm^{-2}. The optimal slope (gradient size) depends on the current density. At low current density a uniform distribution results in maximum performance. At medium and high current densities graded CLs provide better performances. Optimal slopes for the ionomer and platinum loadings vary depending on the load.
-Chen et al.[18] -TP catalyst and ionomer gradients -experimental -spraying	Made DCLs with increasing ionomer and Pt/C ratios towards the membrane using commercial catalysts of 70%, 60%, and 40% Pt/C ratios and Nafion™ contents of 20%, 23%, 24.5%, 33%, and 40%. The total cathode loading was fixed at 0.2 mg cm^{-2} and the samples were investigated at 60 °C at 80% RH and 20% RH using H_2-air. Compared with a sample having an ionomer content of 24.5% and Pt/C ratio of 60%, a DCL with increasing Pt content (from 40% Pt/C to 70% Pt/C) and increasing ionomer content (23% to 33%) to the membrane interface improved the peak power density by 38.4% at 80% RH and by 135.7% at 20% RH.

Table A·1. (Continued).

Specifications	Study and Results
-Yu et al.[15] -TP catalyst gradients -experimental -spraying	Made through-plane gradients in terms of the Pt particle size increasing from 2 to 5 nm towards the membrane. The Pt/C ratio was 40% and the I/C ratios were 1.00. The Pt loading was ∼0.11 mg cm^{-2} for the cathode and the ASTs were conducted at 100% RH and 80 °C by DOE defined triangular wave potential cycling from 0.6 V to 1.0 V for 30,000 cycles at 50 mV s^{-1} scan rate. Increasing the particle size to 5 nm towards the membrane interface resulted in improved durability, less Pt dissolution, and higher ECSA retention compared to 2 nm particles close at the GDL. The performance of the MEA with the gradient was better by 50–100 mV at EOL.
-Yu et al.[16] -TP catalyst gradients -experimental -spraying	Used 2 nm Pt particles to make an increasing Pt loading gradient towards the membrane by using Pt/C ratio of 60 % near the membrane interface and 40% at the GDL interface. The overall Pt loading was ∼0.11 mg cm^{-2} for the cathode and the I/C ratios were 1.00. ASTs were conducted at 100% RH and 80 °C by DOE defined triangular wave potential cycling from 0.6 V to 1.0 V for 30,000 cycles at 50 mV s^{-1} scan rate. Performance at BOT and EOT was improved by ∼100 mV for the gradient due to less Pt loss in the depletion zone (from 80% to 60%).
-Roh et al.[67] -TP catalyst and binder gradients -experimental Spraying	Synthesized Pt/C nanoparticles with oxygen-functionalized carbon supports having a Pt content of 20% to make DCLs with hydrophilic layer close to membrane and hydrophobic layer close to the GDL (using the non-functionalized catalyst). The DCL was compared with a commercial Pt/C catalyst (20% Pt/C) and the total Pt loading was 0.2 mg cm^{-2} for the samples. The Pt loading for the DCL was equally distributed and the ionomer content was at 35 wt%. The samples were tested at 50 °C, and RH of ∼26% with a backpressure of 1.8 bar, in H_2-air. Using DCL at both anode and cathode resulted in a maximum power density of ∼610 mW cm^{-2} whereas the unform samples had maximum power densities close to ∼430 mW cm^{-2}.
-Shahgaldi et al.[35] -TP catalyst and ionomer gradients -experimental -spraying	Made DCLs using a 60% Pt/C catalyst and a 790 $g_{polymer}$ $mol^{-1}_{SO_3^{-1}}$ ionomer by making two layers with different Pt loading and ionomer contents. The total cathode Pt loading was fixed to 0.4 mg cm^{-2}, and the samples were tested at 75 °C, 35 kPag, with H_2-air at 100% RH. Placing 0.3 mg cm^{-2} at GDL interface with an I/C ratio of ∼0.45 and 0.1 mg cm^{-2} at the membrane interface with an I/C ratio of ∼1.1 resulted in a peak power performance of ∼1.24 W cm^{-2}. Non-graded samples with I/C ratios of ∼0.45, ∼0.83, and ∼1.25 resulted in lower peak power densities of 0.96 W cm^{-2}, 1.10 W cm^{-2}, and 0.93 W cm^{-2} respectively. An equal catalyst distribution among the layers with the same ionomer loading distribution as the optimum DCL resulted in a peak power density of ∼1 W cm^{-2}.
-Baricci et al.[17] -TP catalyst gradients -numerical + experimental -spraying	Studied the Pt dissolution rates of gradients increasing to the membrane for Pt particle sizes (from 2 to 5 nm) and Pt/C ratios (40% Pt/C to 60% Pt/C). The gradients were compared to homogenous samples having Pt particle size of 2, 3 and 5 nm (40% Pt/C), and the I/C ratios of 1.00. The Pt loading was ∼0.11 mg cm^{-2} and the ASTs were conducted at 100% RH and 80 °C by DOE defined triangular wave potential cycling from 0.6 V to 1.0 V for 30,000 cycles at 50 mV s^{-1} scan rate. The authors found that samples with smaller particles initially displayed higher ECSA and catalyst utilization factors but also had higher catalyst depletion rates at the membrane interface. CLs with larger particles close to the membrane showed a lower relative change of ECSA after 30,000 potential sweeps and less Pt dissolution due to Ostwald ripening. A similar scenario was observed for the gradient with higher Pt/C ratio at the membrane interface.
-Xing et al.[144] -IP catalyst gradients -numerical + experimental -spraying	Used a series of equations based on conservation laws such as for mass, momentum and heat to investigated the influence of the GDL porosity and in-plane catalyst gradients on the cell performance and current distribution. Platinum loadings of 0.1, 0.2, and 0.4 mg cm^{-2} were used (40% Pt/C ratio) and an I/C ratio of 0.7. The simulations and experiments were done at 60 °C, 0.1 MPa, and 100% RH with H_2-air. Having GDLs with higher porosities of ∼0.6 at the outlet and ∼0.2 at the inlet (equal distribution) results in ∼ 100 mV improvement at 1.3 A cm^{-2} (max. current density) compared to the opposite grading direction. The catalyst distribution didn't show differences when the porosity was higher at the outlet. However, when the porosity was higher at the inlet, placing, 0.2 mg cm^{-2} at the inlet, and 0.4 mg cm^{-2} at the outlet resulted in worse performances than the opposite platinum distribution direction. Systematically controlling the loading and GDL porosity can simultaneously improve the cell performance and homogenize the current density distribution. However, the optimal distribution for the loading depends on the operating conditions and the GDL porosity in turn.
-Wang et al.[145] -TP and IP ionomer gradients -numerical	Used a three-dimensional multiphase model verified with experimental data from another study to investigate cell performance for various RHs and dry ionomer volume fractions. The model assumed an operating temperature of 80 °C and Pt loadings of 0.4 mg cm^{-2} (40% Pt/C). The ionomer dry volume fractions were varied between 0.1 and 0.4 (in steps of 0.05) and the RH between 100% RH and 40% RH (in steps of 20%). At 100% RH the optimum performance was for ionomer volume fractions of 0.2 and 0.25, whereas at 40% RH, the optimum was for 0.4. Using a linear TP gradient from 0 to 0.5 or from 0.1 to 0.4 results in a maximum power density of ∼600 mW cm^{-2} at 60% RH whereas a homogenous layer with 0.2 results in ∼580 mW cm^{-2}. Opposite gradients result in worse performances. Placing a slightly higher dry volume fraction of the ionomer towards the outlet (0.1 to 0.4 or 0.2 to 0.3) results in similar performances compared with a homogenous layer with 0.2 volume fraction, whereas bigger gradients result in worse performances.

Table A·1. (Continued).

Specifications	Study and Results
-Zheng et al.[14] -TP catalyst gradients -numerical	A mathematical model was used to investigate the potential benefits of Pt particle size gradients on catalyst layer durability. Using Pt particle sizes, about 4–5 nm near the membrane, could mitigate ECSA losses by 33 to 55 % compared to particle sizes of 3 nm. This could, however, accelerate the Pt dissolution at the GDL interface, despite reducing the Pt dissolution at the membrane interface. A TCL with a smoother transition (5–4–3 nm) was recommended to counterbalance this effect, along with an increasing loading gradient towards the GDL.
-Lin et al.[12] -TP binder gradients -experimental -decal transfer	Made multiple trilayers and DCLs for a MEAs with PTFE having I/C ratios of 0.8 while fixing the Pt loading (50% Pt/C) at 0.2 mg cm^{-2} for the cathode. The samples were tested at 80 °C, 0.3 bar, and 100% RH with H_2-air, and the ASTs were done by voltage cycling between 0.6 and 1.0 V with H_2-N_2 at a scan speed of 50 mV s^{-1}. Additionally, performance data were acquired at 70% RH and 30% RH, and 0.3 and 0.6 bar. Authors conclude that there is an optimum PTFE content (around 10 wt%) for improved durability and performances depending on operating conditions, preferentially applied to the outer layer close to the GDL. Compared to a non-graded sample, the improvement can improve by ∼30% in peak power density. An optimum tri-layer does not result in greater improvements compared to the double catalyst layer with the same PTFE content in the outer layer.
-Garsany et al.[68] -TP catalyst gradients -experimental -spray coating	Made DCLs with two different catalysts, Ketjenblack and Vulcan type catalysts (both 40% Pt/C), to make pore size and catalyst gradients. The total Pt loading for the cathode was fixed at 0.25 mg cm^{-2} and an I/C ratio of ∼0.6 was used. The samples were tested at 80 °C, ambient pressure, RHs of 100% and 25% with H_2-air. At 100% RH, there was no noticeable difference between graded MEAs and homogenously coated samples. At an RH of 25% placing two well defined layers of the separate catalysts (either Ketjenblack Pt/C first or Vulcan Pt/C first) resulted in almost 18% improvement in peak power density regardless of the order in which the layers are placed. However, blending the two catalysts inks resulted in similar performance as the non-graded samples at both RHs.
-Xing et al.[146] -IP catalyst gradients -numerical + experimental	Graded a cell with decreasing Pt content and increasing temperature from the cathode inlet towards the outlet. The cathode Pt loading was 0.4 mg cm^{-2} (40% Pt/C) and the I/C ratio was fixed at 1.5. H_2-air was used in a segmented fuel cell with 100% RH at atmospheric pressure. Increasing the temperature from 35 °C (inlet) to 65 °C (outlet) while utilizing 0.4 mg cm^{-2} at the inlet and 0.25 mg cm^{-2} at the outlet can result in ∼260% improvement in current density at 0.6 V and ∼70% at 0.3 V while resulting in ∼18% reduction in Pt loading. Increased temperature at outlet decreased liquid water content and increased effective oxygen diffusion coefficient and reaction rate.
-Nguyen et al.[33] -TP catalyst and ionomer gradients -experimental -spraying	Graded MEAs in the through-plane direction with non-fluorinated ionomers. Low I/C ratios of 0.2, 0.4, and 0.5 were investigated for the low EW ionomer (EW ≈333) and the total Pt loading was fixed at 0.4 mg cm^{-2} for the cathode. Polarization curve measurements were made at 95 °C, 250 kPa, 80% and 50% RH using H2-air. For the catalyst distribution, an increasing catalyst loading towards the GDL (75% of catalyst at the GDL interface, and 25% at membrane interface) is found to be the optimum distribution while increasing the ionomer content towards the membrane (I/C ratios of 0.2 and 0.4).

ORCID

Marc Ayoub https://orcid.org/0009-0001-9977-254X
Thomas Böhm https://orcid.org/0000-0003-2036-2159
Simon Thiele https://orcid.org/0000-0002-4248-2752
Matthew Brodt https://orcid.org/0000-0002-6895-9889

References

1. IEA, (2023), Electrolysers - Energy Systems https://www.iea.org/energy-system/low-emission-fuels/electrolysers.
2. Straits Research, "Water Electrolysis Market Size, Share & Trends Analysis Report By Electrolyzer Type (Alkaline Electrolyzer, Proton Exchange Membrane (PEM) Electrolyzer, Solid Oxide Electrolyzer Cell (SOEC), Anion Exchange Membrane (AEM) Electrolyzer), By End-User Applications (Ammonia Production, Methanol Production, Refining Industry, Power and Energy Storage, Transportation/Mobility Industry, Others) and By Region(North America, Europe, APAC, Middle East and Africa, LATAM) Forecasts, 2024-2032." *Water Electrolysis Market SRAP54095DR* (04, March 2024), https://straitsresearch.com/report/water-electrolysis-market.
3. (2021), E4tech. E4tech Fuel Cell Industry Review 2020.2 https://www.erm.com/solutions/climate-net-zero/the-fuel-cell-industry-review/.
4. T. Bednarek, J. Davies, T. Malkow, and E. Weidner, *Historical Analysis of FCH 2 JU Stationary Fuel Cell Projects*, Publications Office of the European Union (2021), JRC125018, https://publications.jrc.ec.europa.eu/repository/handle/JRC125018.
5. "A SUSTAINABLE PATHWAY FOR THE EUROPEAN ENERGY TRANSITION." *Hyrogen Roadmap Europe*, Fuel Cells and Hydrogen 2 Joint Undertaking (2019).
6. *Addendum to the Multi - Annual Work Plan 2014 - 2020* (2018), https://www.clean-hydrogen.europa.eu/ FUEL CELLS and HYDROGEN 2 JOINT UNDERTAKING (FCH 2 JU).
7. "US Driving research and innovation for vehicle efficiency and energy sustainability." *Fuel Cell Technical Team Roadmap* (2017), https://www.energy.gov/eere/vehicles/us-drive U.S. Department of Energy.
8. M. Breitwieser, M. Klingele, S. Vierrath, R. Zengerle, and S. Thiele, "Tailoring the Membrane-Electrode Interface in PEM Fuel Cells: A Review and Perspective on Novel Engineering Approaches." *Advanced Energy Materials*, **8**, 1701257 (2017).
9. *Handbook of Fuel Cells: Fundamentals, Technology, Applications*Wolf Vielstich, Arnol Lamm, and Hubert Gasteiger (ed.), (Wiley, New York) 4, 631 (May 2003).
10. A. Damjanovic and V. Brusic, "Electrode kinetics of oxygen reduction on oxide-free platinum electrodes." *Electrochim. Acta*, **12**, 615 (1967).
11. D. Gidaspow, "Handbook of fuel cell technology, carl berger, editor, prentice-hall, englewood cliffs, N. J. (1968). 607 pages. $18.50." *AIChE J.*, **15**, 3 (1969).
12. R. Lin, H. Wang, and Y. Zhu, "Optimizing the structural design of cathode catalyst layer for PEM fuel cells for improving mass-specific power density." *Energy*, **221**, 119909 (2021).
13. K.-H. Kim, H.-J Kim, K.-Y. Lee, J. H. Jang, S.-Y. Lee, E. Cho, I.-H. Oh, and T.-H. Lim, "Effect of Nafion® gradient in dual catalyst layer on proton exchange membrane fuel cell performance." *Int. J. Hydrogen Energy*, **33**, 2783 (2008).
14. Z. Zheng, Y. Fan, L. Chen, Z. Fengjuan, S. Shuiyun, W. Guanghua, and Z. Junliang, "Design of gradient cathode catalyst layer (CCL) structure for

mitigating Pt degradation in proton exchange membrane fuel cells (PEMFCs) using mathematical method." *J. Power Sources*, **451**, 227729 (2020).
15. H. Yu, A. Baricci, A. Bisello, A. Casalegno, L. Guetaz, L. Bonville, and R. Maric, "Strategies to mitigate Pt dissolution in low Pt loading proton exchange membrane fuel cell: I. A gradient Pt particle size design." *Electrochim. Acta*, **247**, 1155 (2017).
16. H. Yu, A. Baricci, A. Casalegno, L. Guetaz, L. Bonville, and R. Maric, "Strategies to mitigate Pt dissolution in low Pt loading proton exchange membrane fuel cell: II. A gradient Pt loading design." *Electrochim. Acta*, **247**, 1169 (2017).
17. A. Baricci, M. Bonanomi, H. Yu, L. Guetaz, R. Maric, and A. Casalegno, "Modelling analysis of low platinum polymer fuel cell degradation under voltage cycling: Gradient catalyst layers with improved durability." *J. Power Sources*, **405**, 89 (2018).
18. G.-Y. Chen, C. Wang, Y.-J. Lei, J. Zhang, Z. Mao, Z.-Q. Mao, J.-W. Guo, J. Li, and M. Ouyang, "Gradient design of Pt/C ratio and Nafion content in cathode catalyst layer of PEMFCs." *Int. J. Hydrogen Energy*, **42**, 29960 (2017).
19. L. Xing, W. Shi, H. Su, Q. Xu, P. K. Das, B. Mao, and K. Scott, "Membrane electrode assemblies for PEM fuel cells: a review of functional graded design and optimization." *Energy*, **177**, 445 (2019).
20. W. Vielstich, H. A. Gasteiger, and H. Yokokawa, *Handbook of Fuel Cells: Fundamentals Technology and Applications* (Wiley, New York) (2009).
21. R. K. F. Della Bella, B. M. Stühmeier, and H. A. Gasteiger, "Universal correlation between cathode roughness factor and H_2/air performance losses in voltage cycling-based accelerated stress tests." *J. Electrochem. Soc.*, **169**, 44528 (2022).
22. Tim van Cleve et al., "Dictating Pt-based electrocatalyst performance in polymer electrolyte fuel cells, from formulation to application." *ACS Appl. Mater. Interfaces*, **11**, 46953 (2019).
23. S. A. Mauger et al., "Influence of ink formulation and drying conditions on ionomer distribution in high-performance roll-to-roll-coated gas-diffusion electrodes." *Meet Abstr.*, **MA2020-02**, 2218 (2020).
24. D. K. Makepeace, A. Fortini, P. Locatelli, C. Lindsay, S. Moorhouse, R. Lind, P. Sear, and J. L. Keddie, "Stratification in binary colloidal polymer films: experiment and simulations." *Soft Matter.*, **13**, 6969 (2017).
25. C. M. Cardinal, Y. D. Jung, K. H. Ahn, and L. F. Francis, "Drying regime maps for particulate coatings." *AIChE J.*, **56**, 2769 (2010).
26. D. Gerteisen, "Impact of inhomogeneous catalyst layer properties on impedance spectra of polymer electrolyte membrane fuel cells." *J. Electrochem. Soc.*, **162**, F1431 (2015).
27. T. Reshetenko and A. Kulikovsky, "Impedance spectroscopy study of the PEM fuel cell cathode with nonuniform nafion loading." *J. Electrochem. Soc.*, **164**, E3016 (2017).
28. H. Nakajima, K. Matsutani, T. Kaieda, and T. Tada, "Effect of the content of platinum and carbon support in cathode catalyst on the cell performance under low and high relative humidity." *ECS Trans.*, **41**, 2049 (2011).
29. E. J. F. Dickinson and G. Hinds, "The butler-volmer equation for polymer electrolyte membrane fuel cell (PEMFC) electrode kinetics: a critical discussion." *J. Electrochem. Soc.*, **166**, F221 (2019).
30. L. Xing, W. Shi, P. K. Das, and K. Scott, "Inhomogeneous distribution of platinum and ionomer in the porous cathode to maximize the performance of a PEM fuel cell." *AIChE J.*, **63**, 4895 (2017).
31. Q. Wang, M. Eikerling, D. Song, Z. Liu, T. Navessin, Z. Xie, and S. Holdcroft, "Functionally graded cathode catalyst layers for polymer electrolyte fuel cells." *J. Electrochem. Soc.*, **151**, A950 (2004).
32. Z. Xie, T. Navessin, K. Shi, R. Chow, Q. Wang, D. Song, B. Andreaus, M. Eikerling, Z. Liu, and S. Holdcroft, "Functionally graded cathode catalyst layers for polymer electrolyte fuel cells." *J. Electrochem. Soc.*, **152**, A1171 (2005).
33. H. Nguyen, D. Sultanova, P. A. Heizmann, S. Vierrath, and M. Breitwieser, "Improving the efficiency of fully hydrocarbon-based proton-exchange membrane fuel cells by ionomer content gradients in cathode catalyst layers." *Mater Adv.*, **23**, 8460 (2022).
34. Y.-G. Yoon, T.-H. Yang, G.-G. Park, W.-Y. Lee, and C.-S. Kim, "A multi-layer structured cathode for the PEMFC." *J. Power Sources*, **118**, 189 (2003).
35. S. Shahgaldi, A. Ozden, X. Li, and F. Hamdullahpur, "Cathode catalyst layer design with gradients of ionomer distribution for proton exchange membrane fuel cells." *Energy Convers. Manage.*, **171**, 1476 (2018).
36. M. M. Saleh, T. Okajima, M. Hayase, F. Kitamura, and T. Ohsaka, "Exploring the effects of symmetrical and asymmetrical relative humidity on the performance of H2/air PEM fuel cell at different temperatures." *J. Power Sources*, **164**, 503 (2007).
37. H. Xu, H. R. Kunz, and J. M. Fenton, "Analysis of proton exchange membrane fuel cell polarization losses at elevated temperature 120°C and reduced relative humidity." *Electrochim. Acta*, **52**, 3525 (2007).
38. Q. Yan, H. Toghiani, and J. Wu, "Investigation of water transport through membrane in a PEM fuel cell by water balance experiments." *J. Power Sources*, **158**, 316 (2006).
39. D. Song, Q. Wang, Z. Liu, M. Eikerling, Z. Xie, T. Navessin, and S. Holdcroft, "A method for optimizing distributions of Nafion and Pt in cathode catalyst layers of PEM fuel cells." *Electrochim. Acta*, **50**, 3347 (2005).
40. P. Jain, L. T. Biegler, and M. S. Jhon, "Optimization of polymer electrolyte fuel cell cathodes." *Electrochem. Solid-State Lett.*, **11**, B193 (2008).
41. F. C. Cetinbas, S. G. Advani, and A. K. Prasad, "Investigation of a polymer electrolyte membrane fuel cell catalyst layer with bidirectionally-graded composition." *J. Power Sources*, **270**, 594 (2014).
42. R. Roshandel and F. Ahmadi, "Effects of catalyst loading gradient in catalyst layers on performance of polymer electrolyte membrane fuel cells." *Renewable Energy*, **50**, 921 (2013).
43. H.-N. Su, Q. Zeng, S.-J. Liao, and Y.-N. Wu, "High performance membrane electrode assembly with ultra-low platinum loading prepared by a novel multi catalyst layer technique." *Int. J. Hydrogen Energy*, **35**, 10430 (2010).
44. M. Srinivasarao, D. Bhattacharyya, and R. Rengaswamy, "Optimization studies of a polymer electrolyte membrane fuel cell with multiple catalyst layers." *J. Power Sources*, **206**, 197 (2012).
45. M. Srinivasarao, D. Bhattacharyya, R. Rengaswamy, and S. Narasimhan, "Performance analysis of a PEM fuel cell cathode with multiple catalyst layers." *Int. J. Hydrogen Energy*, **35**, 6356 (2010).
46. M. Secanell, K. Karan, A. Suleman, and N. Djilali, "Multi-variable optimization of PEMFC cathodes using an agglomerate model." *Electrochim. Acta*, **52**, 6318 (2007).
47. M. Secanell, R. Songprakorp, N. Djilali, and A. Suleman, "Optimization of a proton exchange membrane fuel cell membrane electrode assembly." *Struct Multidisc Optim.*, **40**, 563 (2010).
48. R. M. Darling and J. P. Meyers, "Kinetic model of platinum dissolution in PEMFCs." *J. Electrochem. Soc.*, **150**, A1523 (2003).
49. E. F. Holby, W. Sheng, Y. Shao-Horn, and D. Morgan, "Pt nanoparticle stability in PEM fuel cells: influence of particle size distribution and crossover hydrogen." *Energy Environ. Sci.*, **2**, 865 (2009).
50. B. Zhao, L. Sun, R. Ran, and Z. Shao, "Design and investigation of dual-layer electrodes for proton exchange membrane fuel cells." *Solid State Ionics*, **262**, 313 (2014).
51. X. Zhang and P. Shi, "Dual-bonded catalyst layer structure cathode for PEMFC." *Electrochem. Commun.*, **8**, 1229 (2006).
52. Z. Xiong, S. Liao, D. Dang, X. Tian, S. Hou, F. Liu, H. Peng, and Z. Fu, "Enhanced water management in the cathode of an air-breathing PEMFC using a dual catalyst layer and optimizing the gas diffusion and microporous layers." *Int. J. Hydrogen Energy*, **40**, 3961 (2015).
53. Y. Qiu, H. Zhang, H. Zhong, and F. Zhang, "A novel cathode structure with double catalyst layers and low Pt loading for proton exchange membrane fuel cells." *Int. J. Hydrogen Energy*, **38**, 5836 (2013).
54. R.-Q. Fu, J.-J. Woo, S.-J. Seo, J.-S. Lee, and S.-H. Moon, "Sulfonated polystyrene/polyvinyl chloride composite membranes for PEMFC applications." *J. Membr. Sci.*, **309**, 156 (2008).
55. A. Ayad, J. Bouet, and J. F. Fauvarque, "Comparative study of protonic conducting polymers incorporated in the oxygen electrode of the PEMFC." *J. Power Sources*, **149**, 66 (2005).
56. M. Santis, S. A. Freunberger, A. Reiner, and F. N. Büchi, "Homogenization of the current density in polymer electrolyte fuel cells by in-plane cathode catalyst gradients." *Electrochim. Acta*, **51**, 5383 (2006).
57. M. Prasanna, E. A. Cho, H.-J. Kim, I.-H. Oh, T.-H. Lim, and S.-A. Hong, "Performance of proton-exchange membrane fuel cells using the catalyst-gradient electrode technique." *J. Power Sources*, **166**, 53 (2007).
58. Y. Zhang, A. Smirnova, A. Verma, and R. Pitchumani, "Design of a proton exchange membrane (PEM) fuel cell with variable catalyst loading." *J. Power Sources*, **291**, 46 (2015).
59. S. Herden, F. Riewald, J. A. Hirschfeld, and M. Perchthaler, "In-plane structuring of proton exchange membrane fuel cell cathodes: Effect of ionomer equivalent weight structuring on performance and current density distribution." *J. Power Sources*, **355**, 36 (2017).
60. Y. Liu, C. Ji, W. Gu, D. R. Baker, J. Jorne, and H. A. Gasteiger, "Proton conduction in PEM fuel cell cathodes: effects of electrode thickness and ionomer equivalent weight." *J. Electrochem. Soc.*, **157**, B1154 (2010).
61. X. Cheng, C. Wang, G. Wei, X. Yan, S. Shen, C. Ke, F. Zhu, and J. Zhang, "Insight into the effect of pore-forming on oxygen transport behavior in ultra-low Pt PEMFCs." *J. Electrochem. Soc.*, **166**, F1055 (2019).
62. X. Cheng, J. You, S. Shen, G. Wei, X. Yan, and J. Zhang, "An ingenious design of nanoporous nafion film for enhancing the local oxygen transport in cathode catalyst layers of PEMFCs." *Chem. Eng. J.*, **439**, 135387 (2022).
63. A. Fischer, H. Wendt, and R. Zuber, *Gas Diffusion Electrode for Membrane Fuel Cells and Method of Making Same*, Germany (1997), EP-0797265-A3.
64. H.-N. Su, S.-J. Liao, and Y.-N. Wu, "Significant improvement in cathode performance for proton exchange membrane fuel cell by a novel double catalyst layer design." *J. Power Sources*, **195**, 3477 (2010).
65. D.-W. Jung, J.-H. Kim, S.-H. Kim, J.-B. Kim, and E.-S. Oh, "Performance enhancement of polymer electrolyte membrane fuel cells by dual-layered membrane electrode assembly structures with carbon nanotubes." *J. Nanosci. Nanotechnol.*, **13**, 3650 (2013).
66. H.-N. Su, S.-J. Liao, T. Shu, and H.-L. Gao, "Performance of an ultra-low platinum loading membrane electrode assembly prepared by a novel catalyst-sprayed membrane technique." *J. Power Sources*, **195**, 756 (2010).
67. C.-W. Roh, J. Choi, and H. Lee, "Hydrophilic-hydrophobic dual catalyst layers for proton exchange membrane fuel cells under low humidity." *Electrochem. Commun.*, **97**, 105 (2018).
68. Y. Garsany, R. W. Atkinson III, B. D. Gould, R. Martin, L. Dubau, M. Chatenet, and K. E. Swider-Lyons, "Dual-layer catalyst layers for increased proton exchange membrane fuel cell performance." *J. Power Sources*, **514**, 230574 (2021).
69. C.-H. Wan, M.-T. Lin, Q.-H. Zhuang, and C.-H. Lin, "Preparation and performance of novel MEA with multi catalyst layer structure for PEFC by magnetron sputter deposition technique." *Surf. Coat. Technol.*, **201**, 214 (2006).
70. A. D. Taylor, E. Y. Kim, V. P. Humes, J. Kizuka, and L. T. Thompson, "Inkjet printing of carbon supported platinum 3-D catalyst layers for use in fuel cells." *J. Power Sources*, **171**, 101 (2007).
71. H. Matsuda, K. Fushinobu, A. Ohma, and K. Okazaki, "Structural effect of cathode catalyst layer on the performance of PEFC." *JTST*, **6**, 154 (2011).

72. D. Fofana, S. K. Natarajan, J. Hamelin, and P. Benard, "Low platinum, high limiting current density of the PEMFC (proton exchange membrane fuel cell) based on multilayer cathode catalyst approach." *Energy*, **64**, 398 (2014).
73. G. Kim, K. Eom, M. Kim, S. J. Yoo, J. H. Yang, H.-J. Kim, and E. Cho, "Design of an advanced membrane electrode assembly employing a double-layered cathode for a PEM fuel cell." *ACS Appl. Mater. Interfaces*, **7**, 27581 (2015).
74. L. Ye, Y. Gao, S. Zhu, J. Zheng, P. Li, and J. P. Zheng, "A Pt content and pore structure gradient distributed catalyst layer to improve the PEMFC performance." *Int. J. Hydrogen Energy*, **42**, 7241 (2017).
75. R. Baumann, A. Willert, F. Siegel, and A. Kohl, *Method for producing catalyst layers for fuel cells*, GermanyUS20120125211A1 (2009), inventors; BAUMANN REINHARD[DE]; WILLERT ANDREAS[DE]; SIEGEL FRANK[DE]; KOHL ALBERT[DE]; SOLVICORE GMBH & CO KG[DE]. METHOD FOR PRODUCING CATALYST LAYERS FOR FUEL CELLS DE20091023160; EP20090010356;WO2010EP03226. US US2012125211 (A1). May 27, 2010.
76. Y. Garsany, R. Atkinson III, and B. Gould, inventors; US GOV SEC NAVY [US]. MULTI-INTERFACE MEMBRANE ELECTRODE ASSEMBLY US202063039762P;US202117349464. US US2021391589 (A1). June 16, 2021*Multi-interface membrane electrode assembly*, United States, US202103 91589A1 (2021).
77. S. M. Hendricks, T. Herdtle, M. K. Debe, and D. J. Mcclure, United StatesUS20100297526A1 (2010), Catalyst layers to enhance uniformity of current density in membrane electrode assemblies.
78. M. Karulkar, *Layered Catalyst Assembly and Electrode Assembly Employing the Sam*, United StatesUS20110159403A1 (2010), inventor; FORD GLOBAL TECH LLC[US]. Layered Catalyst Assembly and Electrode Assembly Employing the Same US20100715592. US US2011159403 (A1). March 2, 2010.
79. A. Kongkanand, E. L. Thompson, and F. T. Wagner, *Fuel cell with layered electrode*, United StatesUS20110143254A1 (2009).
80. S. Mcdermid, H. Chhina, and D. Manolescu, *Multi-layer fuel cell electrodes with different loadings on the supported catalysts*, United StatesWO2017009703A1 (2016).
81. L. V. Protsailo, L. R. Stolar, J. M. Marzullo, M. Gummalla, and S. F. Burlatsky, *Fuel cell electrode with gradient catalyst structure*, United States US2014035 6757A1 (2012).
82. B. Xu, K. A. Littau, and D. K. Fork, *Method for forming multiple-layer electrode structure for silicon photovoltaic cell*, Japan JP2009231840A (2009).
83. D. J. Kuenne, Japan JP2018144030A (2018), Multi-layer slot die and method.
84. American Coatings Association Clifford Schoff, (19 November 2019), Optimum Viscosity for Paint Application, https://www.paint.org/coatingstech-magazine/articles/optimum-viscosity-paint-application/.
85. Keyence, Shaping the Future of Automation Coating & Dispensing Technology: Industrial Coating Overview. https://keyence.com/ss/products/measure/sealing/production/film-sheet.jsp (24 March 2022).
86. Energy.gov. Chapter 6—QUADRENNIAL TECHNOLOGY REVIEW, an assessment of energy technologies and research opportunities , Innovating Clean Energy Technologies in Advanced Manufacturing, https://energy.gov/downloads/chapter-6-innovating-clean-energy-technologies-advanced-manufacturing (September 2015).
87. I. Fouzaï, S. Gentil, V. C. Bassetto, W. O. Silva, R. Maher, and H. H. Girault, "Catalytic layer-membrane electrode assembly methods for optimum triple phase boundaries and fuel cell performances." *J. Mater. Chem. A*, **9**, 11096 (2021).
88. Sono-Tek Announces New Roll-to-Roll Coating Equipment Development Program—Sono-Tek. https://sono-tek.com/sono-tek-announces-new-roll-to-roll-coating-equipment-development-program/Sono-Tek (2021).
89. Xaar. Ultra High Viscosity Technology | Xaar. https://xaar.com/en/technologies/ultra-high-viscosity-technology/xaar, (2022), Accessed November 11, 2022.
90. Sono-Tek, Spray Shaping Systems, https://sono-tek.com/ultrasonic-coating/spray-shaping-systems | (Published October 5, 2022. Accessed November 11, 2022.).
91. X. Ding, J. Liu, and T. A. L. Harris, "A review of the operating limits in slot die coating processes." *AIChE J.*, **62**, 2508 (2016).
92. Ossila, Slot-Die Coating Theory, Design & Applications. https://ossila.com/pages/slot-die-coating-theory#troubleshooting (Accessed March 28, 2022).
93. E. Shim, "Coating and laminating processes and techniques for textiles." *Smart Textile Coatings and Laminates* (Elsevier, Amsterdam) 11 (2019).
94. FOM Technologies, Slot-die coating | Coating equipment | FOM Technologies. https://fomtechnologies.com/fom-science/technology (Published October 5, 2021. Accessed March 27, 2022).
95. R. R. Søndergaard, M. Hösel, and F. C. Krebs, "Roll-to-Roll fabrication of large area functional organic materials." *J Polym Sci B Polym Phys*, **51**, 16 (2013).
96. *Smart Textile Coatings and Laminates*William C. Smith (ed.), (Elsevier, Amsterdam) (2019).
97. S. Mauger, K. C. Neyerlin, J. Stickel, M. Ulsh, K. More, and D. Wood, *Material-Process-Performance Relationships for Roll-to-Roll Coated PEM Electrodes* (National Renewable Energy Lab. (NREL), Golden, CO (United States)) (2017), NREL/PR-5900-68416. https://osti.gov/biblio/1354769.
98. Ossila, Slot-Die Coating Theory, Design & Applications https://ossila.com/en-eu/pages/slot-die-coating-theory#Neck-In (Accessed August 17, 2023).
99. Christopher Foster, Craig Banks, and Rashig O. Kadara, *Screen-Printing Electrochemical Architectures* (Springer International Publish, Cham, Switzerland) (2015).
100. K. C. Honeychurch and J. P. Hart, "Screen-printed electrochemical sensors for monitoring metal pollutants." *TrAC - Trends in Analytical Chemistry*, **22**, 456 (2003).
101. J. P. Metters, R. O. Kadara, and C. E. Banks, "New directions in screen printed electroanalytical sensors: an overview of recent developments." *Analyst*, **136**, 1067 (2011).
102. Flexible Fluxgate Sensor | Encyclopedia MDPI. https://encyclopedia.pub/item/revision/8ac1e5c120219284195467747ebd78de (Accessed November 11, 2022).
103. Zimmerandpeacock, Pros and Cons of screen printed electrodes https://zimmer-peacocktech.com/2020/11/02/pros-and-cons-of-screen-printed-electrodes/ (2020).
104. P. Izak, J. Mastalska-Poplawska, J. Lis, and A. Stempkowska, "Modification of the rheological properties of screen printing ceramic paints containing gold." *J. Phys. Conf. Ser.*, **790**, 12011 (2017).
105. FOM Technologies, Printing, coating, metering & the slot-die process FOM Technologies https://fomtechnologies.com/insights-blog/printing-coating-metering-the-slot-die-process (Published November 15, 2021. Accessed August 17, 2023).
106. L. Gonzalez-Macia and A. J. Killard, "Screen printing and other scalable point of care (POC) biosensor processing technologies." *Medical Biosensors for Point of Care (POC) Applications*, ed. R. Narayan (Elsevier/Woodhead Publishing, Amsterdam, Netherlands) 69 (2017).
107. T. Sabu and J. Izdebska, *Printing on Polymers* (Elsevier, Amsterdam) (2016).
108. The Pros and Cons of Flexo vs. Gravure Printing - paper, Film & Foil Converter. https://pffc-online.com/print/17081-the-pros-and-cons-of-flexo-vs-gravure-printing (17 October 2022).
109. R. Søndergaard, M. Hösel, D. Angmo, T. T. Larsen-Olsen, and F. C. Krebs, "Roll-to-roll fabrication of polymer solar cells." *Mater. Today*, **15**, 36 (2012).
110. B. A. Morris, *The Science and Technology of Flexible Packaging: Multilayer Films from Resin and Process to End Use* (William Andrew, Amsterdam, Netherlands) (2017).
111. Energy.gov. Advanced Manufacturing Office 2020 Year in Review. Published May 28, 2024. Accessed May 28, 2024. https://energy.gov/eere/ammto/articles/advanced-manufacturing-office-2020-year-review (December 31, 2020).
112. C. Bois, A. Blayo, D. Chaussy, R. Vincent, A.-G. Mercier, and C. Nayoze, "Catalyst layers for PEMFC manufactured by flexography printing process: performances and structure." *Fuel Cells*, **12**, 199 (2012).
113. Rheology Lab, Rheology and Dynamic Wetting Characterisations for Slot Die Processes - Expert Analyses from the Rheology Labhttps://rheologylab.com/articles/coatings-paints-inks/slot-die-coating-rheology/.
114. M. Bodner, H. R. García, T. Steenberg, C. Terkelsen, S. M. Alfaro, G. S. Avcioglu, A. Vassiliev, P. Søren, and H. A. Hjuler, "Enabling industrial production of electrodes by use of slot-die coating for HT-PEM fuel cells." *Int. J. Hydrogen Energy*, **44**, 12793 (2019).
115. (2018), Energy.gov. Development of Real-Time Characterization Tools and Associated Efforts to Assist Membrane Electrode Assembly Manufacturing Scale-Up Webinar. https://energy.gov/eere/fuelcells/articles/development-real-time-characterization-tools-and-associated-efforts-assist.
116. S. A. Mauger, M. Wang, F. C. Cetinbas, M. J. Dzara, J. Park, D. J. Myers, R. K. Ahluwalia, S. Pylypenko, L. Hu, S. Litster, K. C. Neyerlin, and M. Ulsh, "Development of high-performance roll-to-roll-coated gas-diffusion-electrode-based fuel cells." *J. Power Sources*, **506**, 230039 (2021).
117. B. Parida, A. Singh, A. K. K. Soopy, S. Sangaraju, M. Sundaray, S. Mishra, S. F. Liu, and A. Najar, "Recent developments in upscalable printing techniques for perovskite solar cells." *Adv. Sci.*, **9**, e2200308 (2022).
118. S. A. Mauger, K. C. Neyerlin, A. C. Yang-Neyerlin, K. L. More, and M. Ulsh, "Gravure coating for roll-to-roll manufacturing of proton-exchange-membrane fuel cell catalyst layers." *J. Electrochem. Soc.*, **165**, F1012 (2018).
119. C. Bois, P. J. J. Dumont, A. Blayo, R. Vincent, C. Nayoze, and D. Chaussy, "Evaluating the effectiveness of using flexography printing for manufacturing catalyst-coated membranes for fuel cells." *Fuel Cells*, **14**, 614 (2014).
120. H.-J. Streitberger and A. Goldschmidt, *BASF Handbook Basics of Coating Technology* (Vincentz Network GmbH & Co. KG, Hanover, Germany) 3rd revised ed. (2018).
121. Changshun Chen et al., "Screen-printing technology for scale manufacturing of perovskite solar cells." *Adv. Sci.*, **10**, e2303992 (2023).
122. Mark Miller, Slot Die Coating Technology https://slotdies.com/slot-die-coating-technology/ (2014).
123. J. Sharma, X. Lyu, T. Reshetenko, G. Polizos, K. Livingston, J. Li, D. L. Wood III, and A. Serov, "Catalyst layer formulations for slot-die coating of PEM fuel cell electrodes." *Int. J. Hydrogen Energy*, **47**, 35838 (2022).
124. E. B. Creel, K. Tjiptowidjojo, J. A. Lee, K. M. Liivingston, P. R. Schunk, N. S. Bell, A. Serov, and D. L. Wood III, "Slot-die-coating operability windows for polymer electrolyte membrane fuel cell cathode catalyst layers." *J. Colloid Interface Sci.*, **610**, 474 (2022).
125. O. A. Baturina, S. R. Aubuchon, and K. J. Wynne, "Thermal stability in air of Pt/C catalysts and PEM fuel cell catalyst layers." *Chem. Mater.*, **18**, 1498 (2006).
126. H.-J. Lee, M. K. Cho, Y. Y. Jo, K.-S. Lee, H.-J. Kim, E. Cho, S.-K. Kim, D. Henkensmeier, T.-H. Lim, and J. J. Jang, "Application of TGA techniques to analyze the compositional and structural degradation of PEMFC MEAs." *Polym. Degrad. Stab.*, **97**, 1010 (2012).
127. J. Speder, A. Zana, I. Spanos, J. J. Kirkensgaard, K. Mortensen, and M. Arenz, "On the influence of the Pt to carbon ratio on the degradation of high surface area carbon supported PEM fuel cell electrocatalysts." *Electrochem. Commun.*, **34**, 153 (2013).
128. Maja Milosevic, Julius Knöppel, Konrad Ehelebe, Dunia Abbas, and L, ópez, Daniel Escalera , Simon Thiele, and Serhiy Cherevko, "Catalyst dissolution analysis in PEM water electrolyzers during intermittent operation." *Meet Abstr.*, **MA2022-01**, 1369 (2022).

130. J. Lobato, P. Cañizares, M. A. Rodrigo, J. J. Linares, D. Úbeda, and F. J. Pinar, "Study of the catalytic layer in polybenzimidazole-based high temperature PEMFC: effect of platinum content on the carbon support." *Fuel Cells*, **10**, 312 (2010).
131. R. R. Díaz-Morales, R. Liu, E. Fachini, G. Chen, C. U. Segre, A. Martínez, C. Cabrera, and E. S. Smotkin, "XRD and XPS analysis of as-prepared and conditioned DMFC array membrane electrode assemblies." *J. Electrochem. Soc.*, **151**, A1314 (2004).
132. Y. K. Phua, D. T. D. Weerathunga, D. Wu, C. Kim, S. M. Jayawickrama, N. Tanaka, and T. Fujigaya, "Effect of carbon nanotube-based catalyst layer surface roughness on polymer electrolyte membrane fuel cell performance." *Sustainable Energy Fuels*, **6**, 4636 (2022).
133. J. Zhang, G. Yin, Z. Wang, and Y. Shao, "Effects of MEA preparation on the performance of a direct methanol fuel cell." *J. Power Sources*, **160**, 1035 (2006).
134. M. Dehlinger, C. Fauquet, S. Lavandier, O. Aumporn, F. Jandard, V. Arkadiev, A. Njeyoumikhov, and D. Tonneau, "Spatial resolution of confocal XRF technique using capillary optics." *Nanoscale Res. Lett.*, **8**, 271 (2013).
135. S. Koch, P. A. Heizmann, S. K. Kilian, B. Britton, S. Holdcroft, M. Breitwieser, and S. Vierrath, "The effect of ionomer content in catalyst layers in anion-exchange membrane water electrolyzers prepared with reinforced membranes (Aemion+™)." *J. Mater. Chem. A*, **9**, 15744 (2021).
136. S. Koch, L. Metzler, S. K. Kilian, P. A. Heizmann, F. Lombeck, M. Breitwieser, and S. Vierrath, "Toward scalable production: catalyst-coated membranes (CCMs) for anion-exchange membrane water electrolysis via direct bar coating." *Advanced Sustainable Systems*, **7**, 2200332 (2023).
137. Friedemann Hegge, Riko Moroni, Patrick Trinke, Boris Bensmann, Richard Hanke-Rauschenbach, Simon Thiele, and Severin Vierrath, "Three-dimensional microstructure analysis of a polymer electrolyte membrane water electrolyzer anode." *J. Power Sources*, **393**, 62 (2018).
138. S. Komini Babu, H. T. Chung, P. Zelenay, and S. Litster, "Resolving electrode Morphology's impact on platinum group metal-free cathode performance using Nano-CT of 3D hierarchical pore and ionomer distribution." *ACS Appl. Mater. Interfaces*, **8**, 32764 (2016).
139. R. Hiesgen, T. Morawietz, M. Handl, M. Corasaniti, and K. Friedrich, "Atomic force microscopy on cross sections of fuel cell membranes, electrodes, and membrane electrode assemblies." *Electrochim. Acta*, **162**, 86 (2015).
140. O. Antoine, Y. Bultel, P. Ozil, and R. Durand, "Catalyst gradient for cathode active layer of proton exchange membrane fuel cell." *Electrochim. Acta*, **45**, 4493 (2000).
141. D. P. Wilkinson and J. St-Pierre, "In-plane gradients in fuel cell structure and conditions for higher performance." *J. Power Sources*, **113**, 101 (2003).
142. S. Ebrahimi, R. Roshandel, and K. Vijayaraghavan, "Power density optimization of PEMFC cathode with non-uniform catalyst layer by Simplex method and numerical simulation." *Int. J. Hydrogen Energy*, **41**, 22260 (2016).
143. S. Ebrahimi, B. Ghorbani, and K. Vijayaraghavan, "Optimization of catalyst distribution along PEMFC channel through a numerical two-phase model and genetic algorithm." *Renewable Energy*, **113**, 846 (2017).
144. L. Xing, Y. Wang, P. K. Das, K. Scott, and W. Shi, "Homogenization of current density of PEM fuel cells by in-plane graded distributions of platinum loading and GDL porosity." *Chem. Eng. Sci.*, **192**, 699 (2018).
145. Y. Wang, T. Liu, H. Sun, W. He, Y. Fan, and S. Wang, "Investigation of dry ionomer volume fraction in cathode catalyst layer under different relative humilities and nonuniform ionomer-gradient distributions for PEM fuel cells." *Electrochim. Acta*, **353**, 136491 (2020).
146. L. Xing, Y. Xu, Ž. Penga, Q. Xu, H. Su, F. Barbir, W. Shi, and J. Xuan, "A segmented fuel cell unit with functionally graded distributions of platinum loading and operating temperature." *Chem. Eng. J.*, **406**, 126889 (2021).